MAGIC-TDAS 09-02
090721/IOya

MAGIC Data Check program

I. Oya
<oya@gae.ucm.es>
R. De los Reyes
<reyes@gae.ucm.es>
J. L. Contreras
<contrera@gae.ucm.es>
N. Mankuzhiyil
<nijil.mankuzhiyil@uniud.it>
D. Nieto
<nieto@gae.ucm.es>
V. Scapin
<valeria.scapin@uniud.it>

July 21, 2009

Abstract

This document is an overview of the MAGIC data check program. This program carries out a continuous check on the telescope performance and the quality of the data taken.

The so called MAGICDC (MAGIC Data Check) program is launched everyday at 9:00 UT, after the telescope is switched off. It checks all the data recorded during the night by all the subsystems of the telescope, in order to detect problems and solve them as soon as possible. Its last step is the evaluation of the most relevant parameters, that is done by the automatic daily-check task.

In the coming sections we make a brief introduction to the MAGIC experiment, a detailed description of how does the program work and a brief description of all the program output: files and plots.

Contents

1 The MAGIC-I Telescope

MAGIC-I (Major Atmospheric Gamma Imaging Cerenkov) is a 17 m diameter Imaging Atmospheric Cerenkov Telescope (IACT) located at El Roque de los Muchachos in the Canary island of La Palma (28.8ºN, 17.9ºW).

MAGIC-I consists of a set of integrated subsystems and structures necessary for the telescope work. At the telescope place a concrete foundation and a tubular space frame supports the drive motors of an alt/az mounting, a 236 m^2 tessellated reflector, a fine granularity photo-sensor camera and the camera cooling system. The telescope has a control room in a nearby building containing the data acquisition system, the camera and calibration power supplies, the trigger system, the weather station, the GPS-time module, all the subsystems and network computing system, and various auxiliary elements needed for safety and backup.

The second telescope of MAGIC experiment, MAGIC-II, is now in commissioning phase and will soon start to take data regularly.

1.1 La Palma computing and network

The computing system MAGIC telescope site consists of a cluster of computers that constitute an internal network connected to Internet through a firewall (wwwint.magic.iac.es) [4] and an external machine (www.magic.iac.es).

The internal network consists of the PCs of the subsystems and the on-site analysis computers. All the computers save their subsystem data locally, sharing it through NFS access (local mount point in /remote). The subsystems computers (PC1-PC7) are software "clones" with OS Suse 7.2 connect to the internal network at 10/100 Mbytes. The computers used for the on-site analysis (*muxana, muxana{2,3,4,5}*) are also "clones" between them but with Red Hat Enterprise Linux (RHEL) 4.3. Central control reports are stored in the /local disk at PC15 (or /remote/pc15 for the rest of computers), DAQ (Data Acquisition) statistics files are stored at *muxdaq* machine and available at /mnt/raid1/muxdata/check/ and finally raw and reduced data are stored in the raid system directories /mnt/raid1/muxdata and /mnt/raid1/analysis . The five *muxana* and *muxdaq* computers are connected with PC15 and raid system through a high speed Gigabit Ethernet connection. More details on the MAGIC computing system can be obtained at the reference [4]

The data check result plots are published in Internet (only for MAGIC private access) through the www.magic.iac.es machine in the /home/www/html/operations/datacheck directory.

The results can be accessed at the MAGICDC web page at La Palma [13] and also at the MAGIC data center at Port d'Informació Científica PIC [16] (http://magic.pic.es/), where all plots are mirrored and stored.

1.2 MARS

The standard analysis software for MAGIC telescope data is called MARS (Magic Analysis and Reconstruction Software). It is a set of C++ (object-oriented framework) classes based on the well known ROOT package from CERN. Basically it can be run in two modes, either inside the ROOT framework using the specific containers and tasks designed to analyze the MAGIC data, or as compiled programs (MARS executables). Some of these MARS executables contain a Graphical User Interface (GUI).

In order to analyze the MAGIC data in a standard way, MARS executables have been used all through the MAGIC telescope data check chain. The executables used are the following ones, displayed inside diamonds in figure 1:

- MERPP: converts the "raw" and ASCII format of MAGIC subsystems to ROOT package format. The output files have the ".root" extension that will be inherited by the following analysis products.
- CALLISTO: calibrates the data. The calibrated files can be recognized by the "_Y_" characters in their name. Besides the standard root files, it is also able to calibrate directly the "raw" files.
- SHOWPLOT: displays graphical information of the output summary files, and allows to convert this graphical information as Postscript file format (".ps"), as well as other formats like ".pdf", ".png" etc
- STAR: calculates the Hillas parameters. The executable output files an be recognized by the "_I_" characters, and are called star files.

Most of these executables have input cards to modify the analysis parameters. All the input cards have the default name of the executable name followed by the ".rc" extension. This is the case of "callisto.rc" and "star.rc".

The analysis executables, callisto and star, run based on "sequences". A sequence is a .txt file that lists the basic information of a data sample to analyze. To find an example of a sequences, see class MSequence [14].

The MAGICDC program only uses the latest official MARS release versions. Therefore, the data check program is, together with the on-site analysis program [15], the first one to test the latest changes on the MARS software itself.

2 MAGICDC: Telescope Data check

The MAGIC-I telescope consists of several telescope elements, called subsystems, which perform specific tasks within the normal data taking (see sec. 1). The quality of the data depends on the good functioning of the telescope and therefore the performance of these subsystems. The program MAGICDC has been developed to check theses subsystems behavior and functionality. It is executed automatically each morning after data taking ends and extracts all the useful information about the telescope status. For final stage, this information is evaluated by a component of the MAGICDC software called Automatic Data Check (see section 2.6).

The MAGICDC program consists on a set of subprograms (see fig. 1) which carry out four main tasks: the first one is to check the data reported for each telescope subsystem and compiled at .rep files, the second one is to check the DAQ statistics file, the third one is to check the output of the calibration files, and the last one to evaluate the telescope performance.

2.1 Steering scripts

The telescope data check program runs in the *muxana* computer, but can be also run in *muxana{2,3,4,5}* machines if needed, and belongs to the local user *analysis*. The program is located at *muxana* in the *analysis* user home directory at ∼analysis/DataCheck/MAGICDC.

All the results and log files of the programs are saved at the NFS system named *raid2* /mnt/raid2/DataCheck/Data, under different sub-directories, depending on the running job.

The MAGICDC program is managed through the Linux *cron daemon* at *muxana* using the crontab file from user *analysis*, which launches the MAGICDC program.

The *analysis* user crontab files launch two different jobs (C-shell scripts) (fig. 1):

- *hal.csh*: This job is launched daily every 20 minutes from 9:00 a.m to 20:00 p.m (UTC) to look for unfinished MAGICDC jobs.
- *monolith.csh*: Takes care of the on-site analysis of the previous days, checking if it has finished properly. Details on the on-site analysis can be obtained in another document [15].

The cron jobs *hal.csh* is launched giving as third parameter a specific date in the format "<year>_<month>_<day>" (all numerical digits), that in normal operation is the current date.

In a first step the *hal.csh* job calls to the *precheck.csh* script which performs the following checks: PC15 and wwwint computers are switched on, /local directory at *muxana* is available, all the subsystem data are available and which kind of data checks should be done. This last check depends on the subsystem data available and whether any of the data check jobs has been already done and finished properly.

The result of the *precheck.csh* script is always an exit code . In case of the first checks, or if all the data check jobs have finished properly, the program *hal.csh* exits with an error message (different for each exit code) refereing to the last task unable to accomplish. In case of missing data check jobs, the *hal.csh* is launched with the adequate configuration.

Depending on the exit code of the *precheck.csh* script, *hal.csh* calls the *launcher* script with different options:

§1. Type of data check: daq, cc, cal, cmux and prof (not mutually exclusive).

§2. Mode: auto, manual, plot or webpage (exclusive).

§3. Day: "<year>_<month>_<day>"

The *launcher* script is the main script which runs the check jobs for the different kinds of data (§1):

I. Central control data (cc option): *CCDataChecking* script (sec. 2.2).

II. DAQ data (cmux option): *CheckMUX* program (sec. 2.3).

III. Calibration data (cal option): *DAQDataChecking* script (sec. 2.4).

IV. Automatic data check (prof option): *prof* (see sec. 2.6).

The *launcher* script can call any of the jobs mentioned above in one mode from the following list (§2):

- `auto`: corresponds to the process automatically launched by the "cron" daemon everyday at 11:00 UTC. This process activates *hal.csh*, which launches consequently the *launcher* script with the `auto` option.
- `manual`: launches the data check of any day (you must specify the "Day" (§3) option).
- `webpage`: transfers the portable document format (.pdf) files with the result plots to the web page.

- `op`: allows the operator user to launch the MAGICDC scripts at any time. This is specially useful to test how are the systems behaving after hardware updates, without waiting to the end of the night shift.

As an example of how the launcher should be called:

```
$PROGRAM_PATH/launcher daqcccalcmuxprof manual 2009_04_09
```

This command launches the whole datacheck and analysis programs for 2009 April 9th.

While running each job all the log files are written at the MAGICDC program subdirectory called logs/. When each check job is finished, the *launcher* script moves the logs files into the job working directory, it sends (by e-mail) a notification to the MAGICDC program developers ("gae-dc@gae.ucm.es") and copies all the Portable Document Format (.pdf) files into the MAGIC web page at La Palma (see sec. 1.1). Its log file (launcher.out) is written into the MAGICDC program bin/ subdirectory.

All the information shown by the MAGICDC program is checked by the MAGIC *professional daily-checkers* who have to fill a daily report about the MAGIC telescope status and, in case of problems, solutions should be sought and be carried out by the experts and the shifters to solve the problems for the next data taking day.

All the MAGICDC program code can be found at the MAGIC CVS [14].

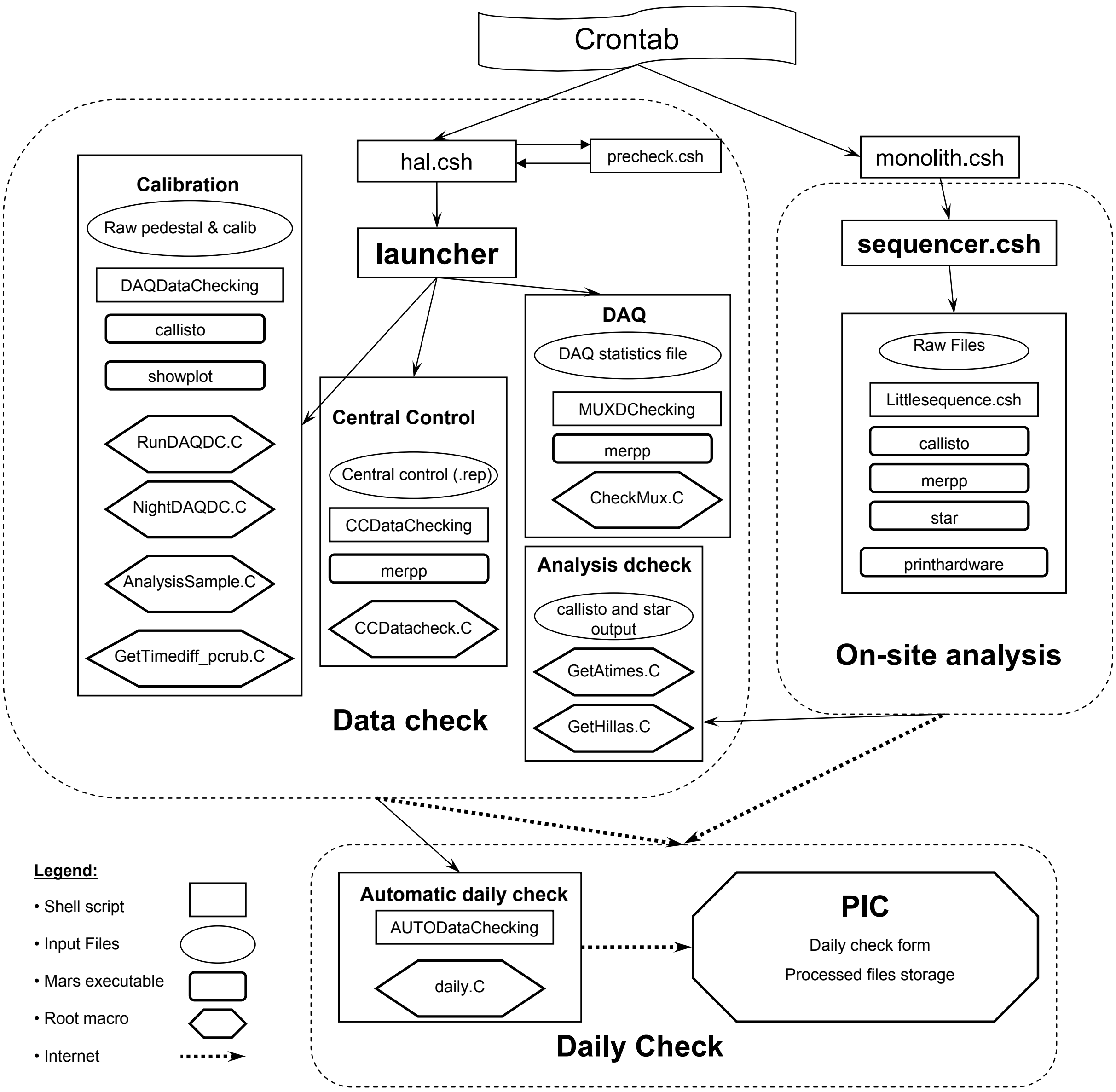

Figure 1: *MAGICDC and on-site analysis programs scheme. After the scripts hal.csh and precheck.csh have confirmed that the computing system is ready, the script launcher will govern the execution of all processes of the different data check sections. Some of the output files generated by the on-site analysis (calib.root, signal.root and star.root) are used as input by the data check program.*

2.2 Central Control data check

The check of the central control data is the first task to be done before any other one. This job checks the performance of all the MAGIC telescope subsystems involved in the data taking, and provides, stogether with the DAQ data check (see sec. 2.3) a first estimation of the night's data quality.

2.2.1 Overview

All the subsystems in the MAGIC site are run and controlled independently by their own programs but they allow the access to most of their functionalities and report all the useful information, through the central control software of the MAGIC telescope (Fig. 2), called SuperArehucas. This software also controls all the the subsystems of the MAGIC-I and MAGIC-II telescopes, which constitute the second phase of the MAGIC experiment.

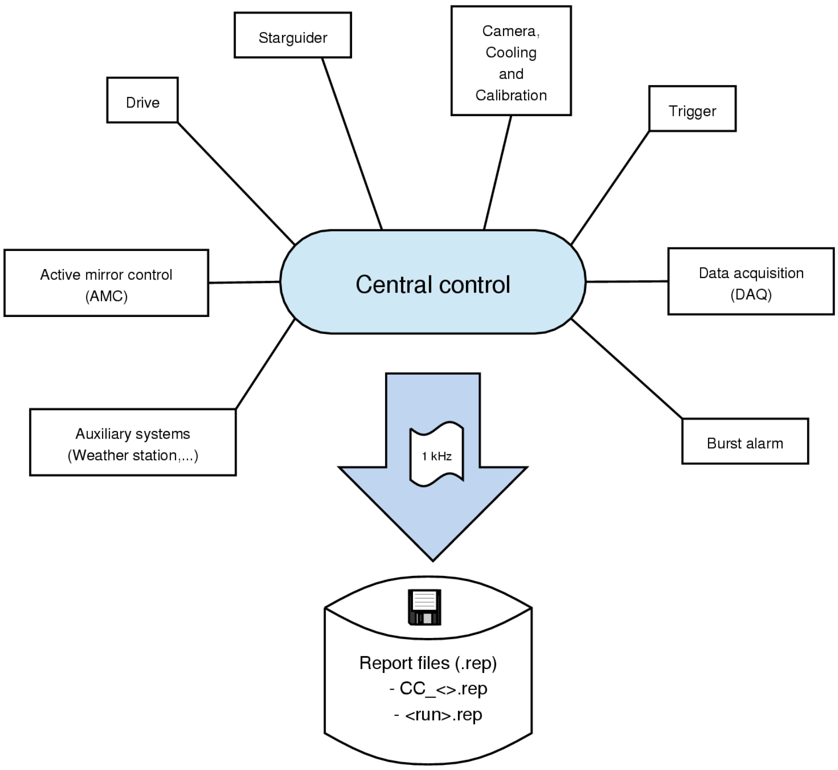

Figure 2: *The MAGIC central control scheme for the normal data taking.*

This program stores, at a rate of 1 kHz, all the subsystems reports in two different kind of ASCII files, both with the extension ".rep". One kind contains the subsystems reports for one subrun, and therefore there is one of these for each, and its name starts with the date of the night. The second kind of file starts with the "CC" characters and keeps all the reports of the subsystems for the whole night. In addition to these reports, specifically sent to the central control, each subsystem could have its own report, log and data check files.

2.2.2 Program

The part of the MAGICDC program which checks the subsystems reports is called by the script *CCDataChecking*. This script joins all the night .rep files (CC_<year>_<month>_<day>.rep), merpps the joined .rep file (CC_<year>_<month>_<day>.root), calls a root macro, *CCDataCheck.C*, to read the generated ".root" file and displays the corresponding subsystems report plots. These plots are classified depending on the subsystem: drive, camera and cooling, trigger, star guider, weather station and time.

The check plots of this part display the information in two different representations: *variable versus time*, to check the variable stability during the night of the subsystem, and *variable versus any other variable* to check previously known correlations between them.

The log file of *CCDataChecking* job, named CCDataChecking_<year>_<month>_<day>.out, is copied, together with the central control results, into the directory
/remote/raid2/analysis/DataCheck/Data/ccdata/<year>_<month>/<year>_<month>_<day>/.

2.2.3 Plots

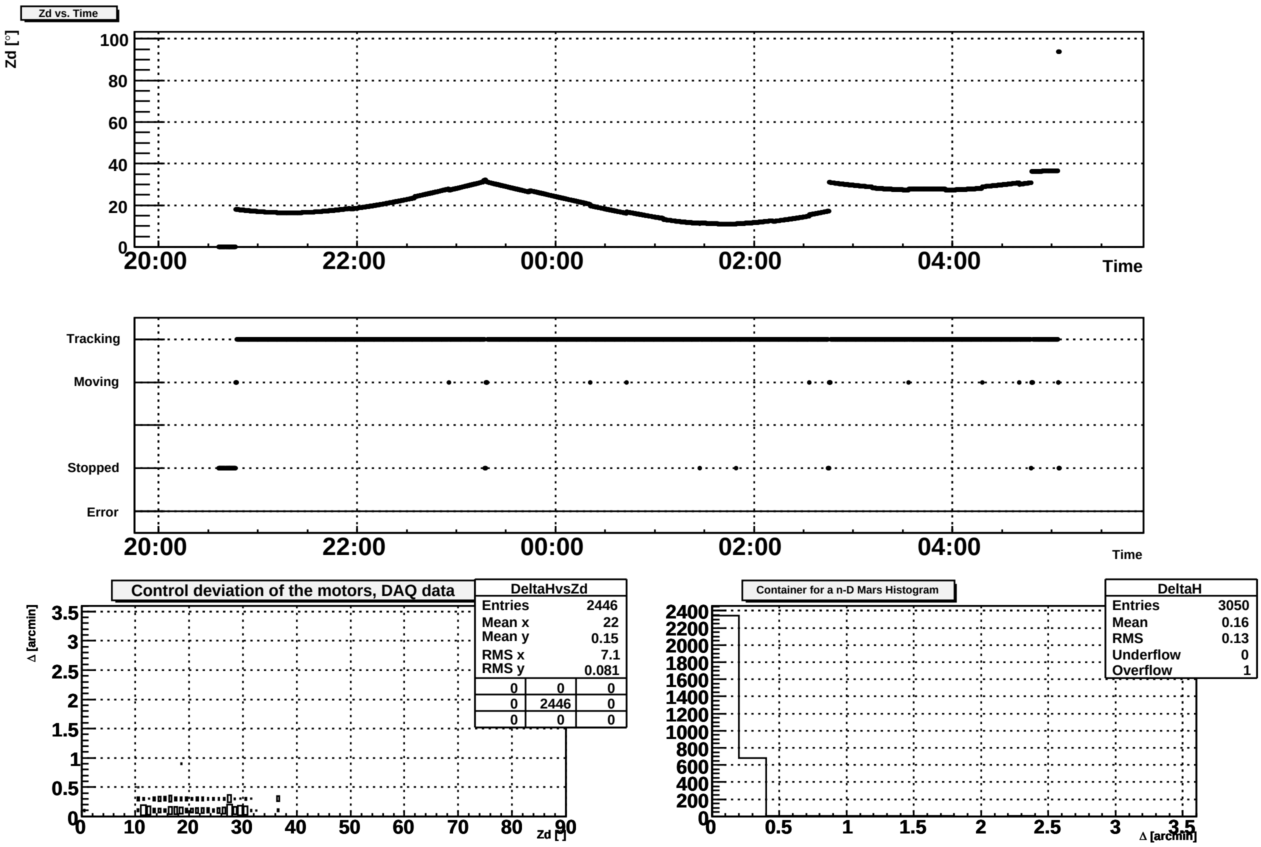

Figure 3: *Drive system report plots. From top to bottom: the zenith angle of the telescope pointing position versus time; the status reported by the system versus time; and the control deviation of the motors (during data taking) versus the zenith angle of pointing position (on the left). The distribution of the control deviation in units of arc-minutes of the motors is shown on the lower right panel).*

Drive Figure 3 shows the plots of the drive system reports. The telescope position in both axes is checked by the shaft encoders. If these plots show that there is a deviation higher than 1.3 arc-minutes this means that the drive is not working properly.

Camera The MAGIC camera is fed with HV (high voltage) by two external power supplies which divide the camera in two halves (A = sectors 1,2,6 and B = sectors 3,4,5). The Camera and Calibration control program (*La Guagua*) evaluates the status of every controlled subsystem (LV, cooling, lid, calibration, etc.) from their regular reports at a given periodicity. A program routine within the Superhareucas program called Sentinel protects the camera against dangerous situations and does not allow certain camera and calibration systems operations [8].

Several plots related to the camera subsystem are produced:

- The status of several monitored elements (PMT high voltages, camera lids, cooling system, PMT direct currents (DC) and camera sentinel) versus time (figure 4).
- The high voltage power supplies and applied direct current as a function of time (figure 5).
- The camera mean high voltage, direct current, and Discrimination Threshold (DT) settings as a function of time (figures 6, 7 and 8). The discrimination threshold settings can be changed along the night by the telescope operators due to different astronomical constrains (moon, twilight) or automatically by the Individual Pixel Rate (IPR) control.
- The applied low voltage and the relative humidity in the LV box as well as its general status and the status of the power supply request, as a function of time (figure 10).
- The high voltage and current of the 360 V active loads and the 175 V power supply of the 5th and 6th PMT dynodes versus time (figure 9).
- The time average of the HV (figure 6) and threshold (figure 8) settings versus the pixel number.

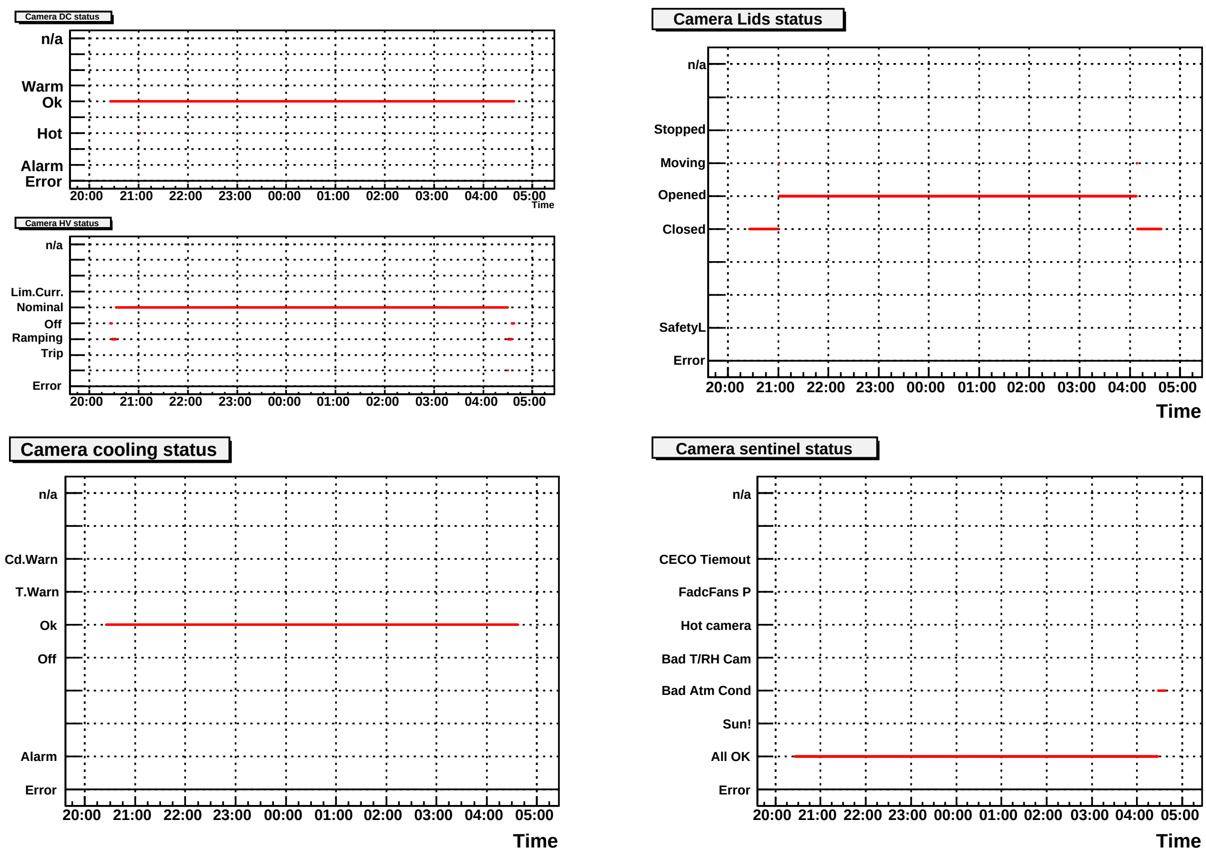

Figure 4: *Camera status report plots. Status plots of the different camera subsystems. Top left: PMT high voltages and DCs. Top right: camera lids. Bottom left: cooling system. Bottom right: camera sentinel.*

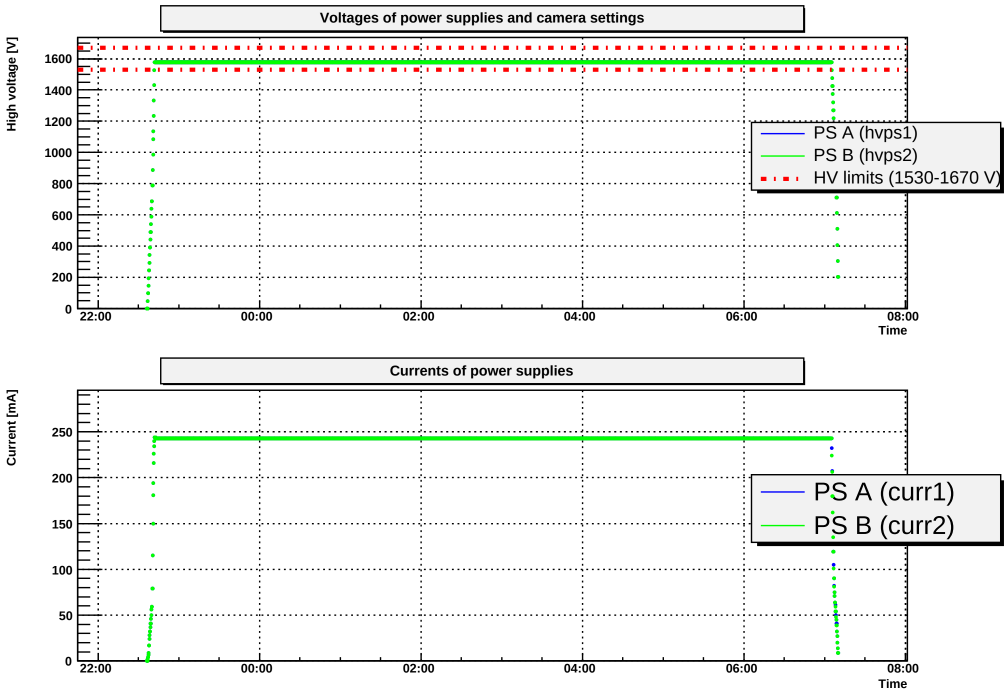

Figure 5: *Power supplies report plots. High voltage and direct current from the power supplies (A, in blue and B, in green). The red-dotted lines are the corresponding limit values for the current HV settings.*

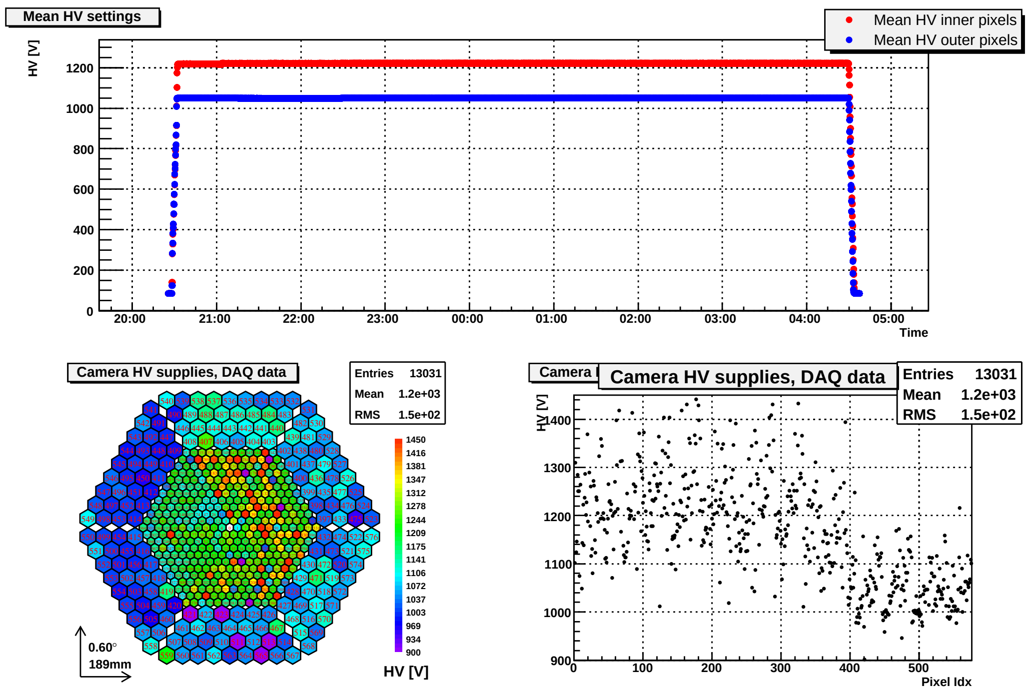

Figure 6: *HV settings report plots. Mean high voltage settings for the whole camera versus time (top) and time average per pixel (bottom).*

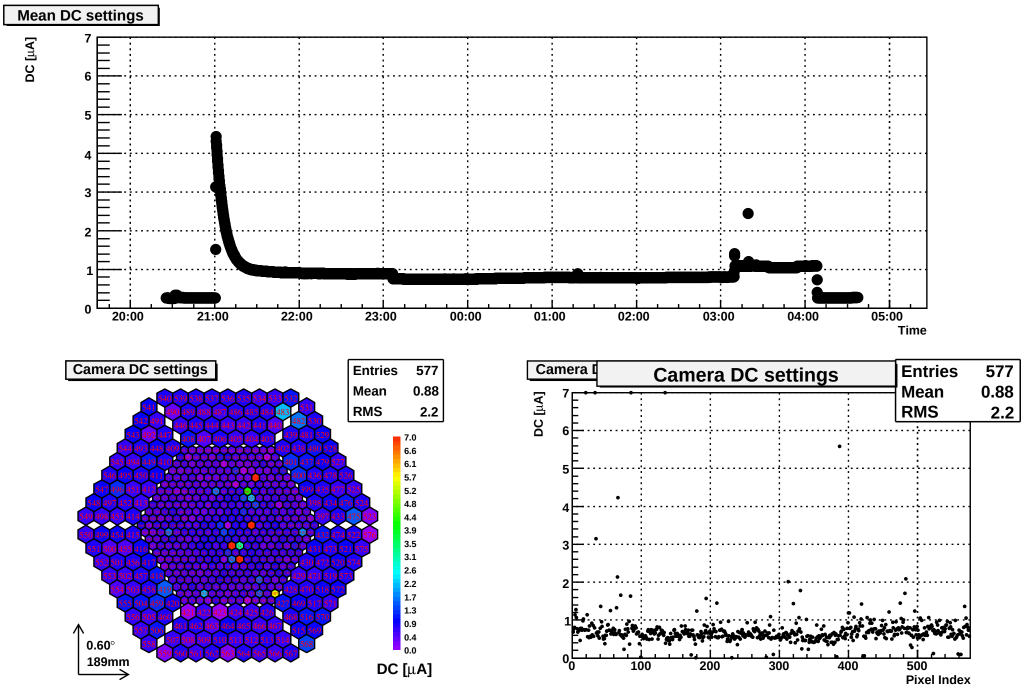

Figure 7: *DC report plots. Mean direct current settings for the whole camera versus time (top) and time average per pixel (bottom).*

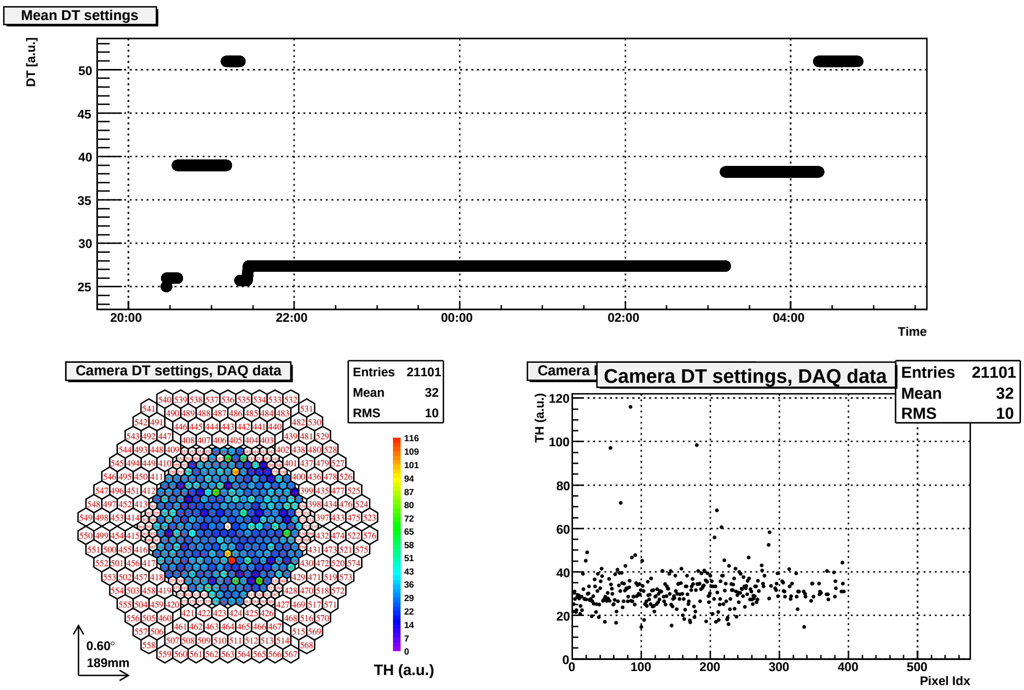

Figure 8: *DT settings report plots. Mean threshold settings for the whole camera versus time (top) and time average per pixel (bottom).*

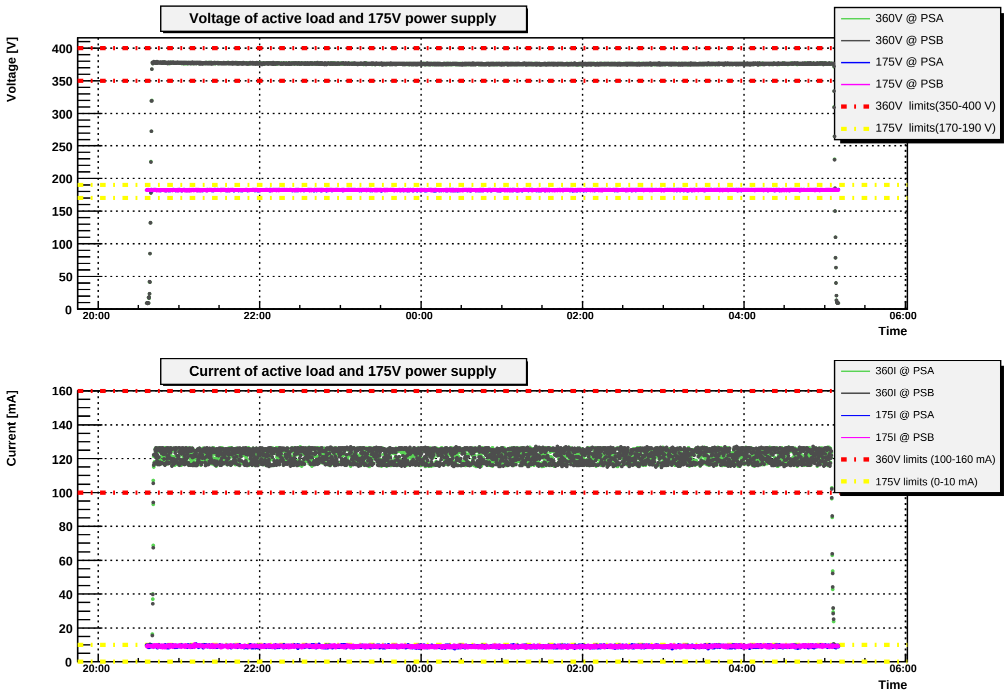

Figure 9: *Active loads report plots. High voltage and direct current applied to 360 V active loads (A (green) and B (grey)), and independent power supply of 175 V (A (blue) and B (pink)). The red-dotted and yellow-dotted lines correspond to the limits to the applied fixed voltages.*

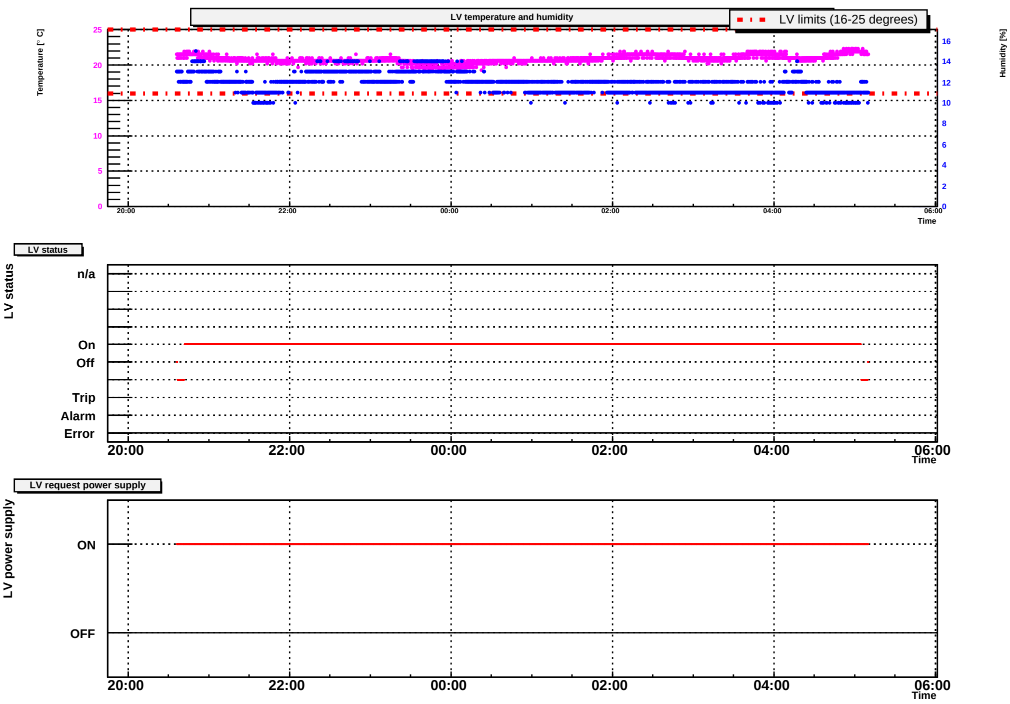

Figure 10: *Low voltage report plots. From top to bottom: Temperature and humidity in the LV box versus time, the status report of the LV system, and the status of the LV power supply.*

Another part of the camera report to the central control concerns the cooling of the camera. To check the cooling system, these plots show the temperature at the center and the walls of the camera, the temperature of the optical links and the water deposit, as well as the relative humidity at the camera center and walls as a function of time. The distribution of the optical links temperature is also displayed but only during the data taking time (figure 11).

The red dashed lines define the range in where the temperature at the center of the camera should lie during the data taking. A temperature outside these limits or with a non stable behavior will have an important effect on the amplification at the optical links. If the temperatures at the optical links and at the camera center differ by more than 2 degrees it means that there is a problem with the fan inside the camera, and therefore that the temperature is not homogeneous. A non homogeneous temperature will cause a different response among the pixels, affecting the camera homogenity.

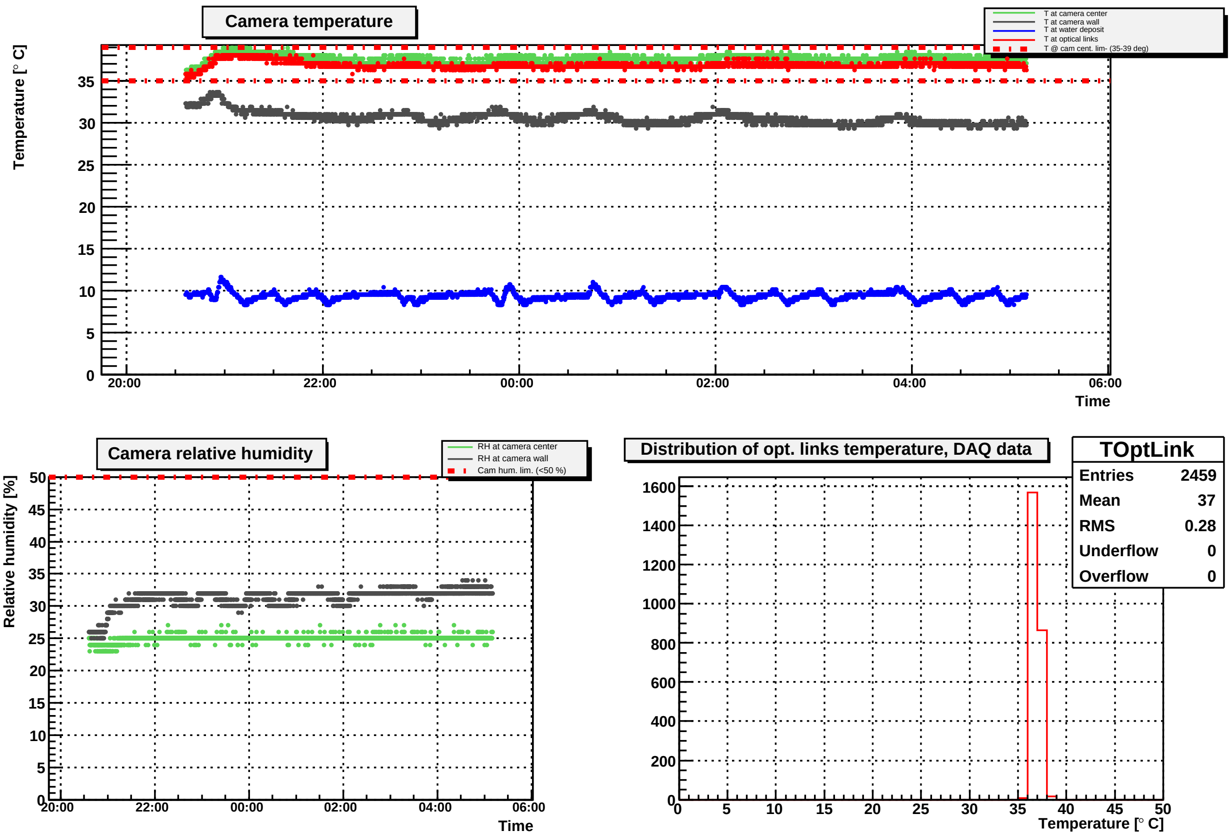

Figure 11: *Cooling system report plots. Top display: temperature versus time of the camera center (green), wall (grey), water deposit (blue) and optical links (red). Bottom left: humidity of the camera at its center (green) and walls (grey). Bottom right: distribution of the optical links temperature during the data taking.*

Trigger Figures 12 and 13 show the first and second level trigger rate versus time, the second level trigger rate versus zenith angle and the night-mean (and RMS) of the IPR per pixel. Figure 14 also shows information about the IPR: the integral and differential distribution of the rate over the number of pixels. If more that 50 pixels have a rate lower that 60 kHz, or more that 10 pixels a rate above 5 MHz, this may indicate that the DTs have been set incorrectly or that the ambient light is too strong. Additionally, if a large number of pixels show too low or too high IPR, it may also be that the HVs have been set incorrectly or that the IPR is not working properly.

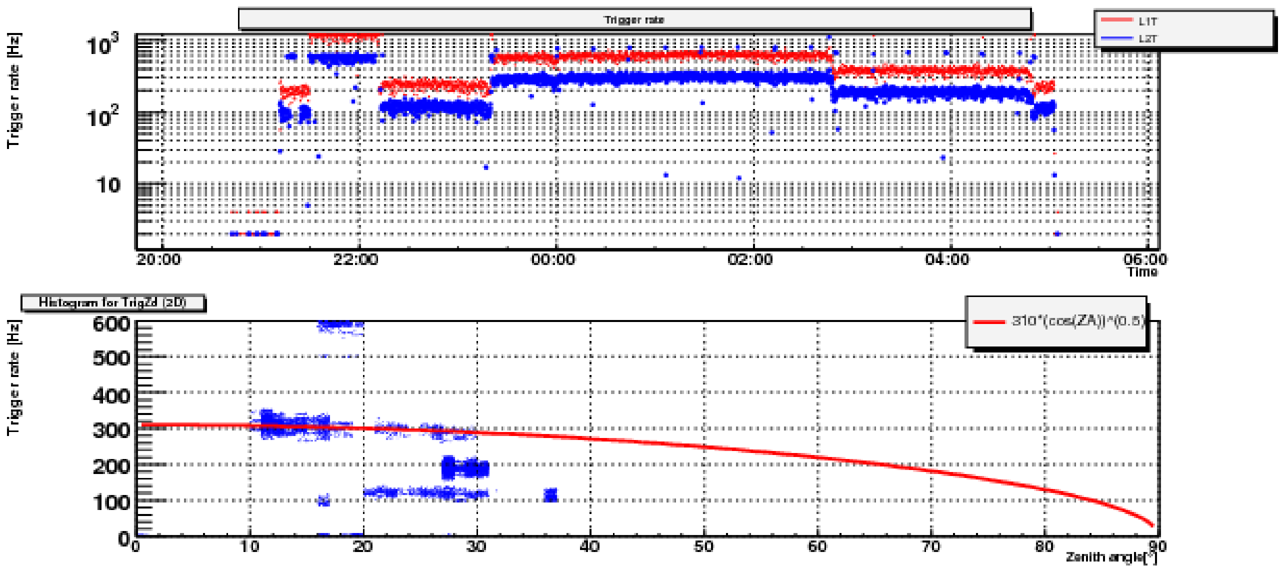

Figure 12: *L1T and L2T report plots. Top: L1T (red) and L2T (blue) rate (Hz) versus time. Bottom: L2T rate (Hz) versus pointing zenith angle (deg) during data taking. The red line corresponds to the expected L2T rate (interlaced events included) for the different zenith angles.*

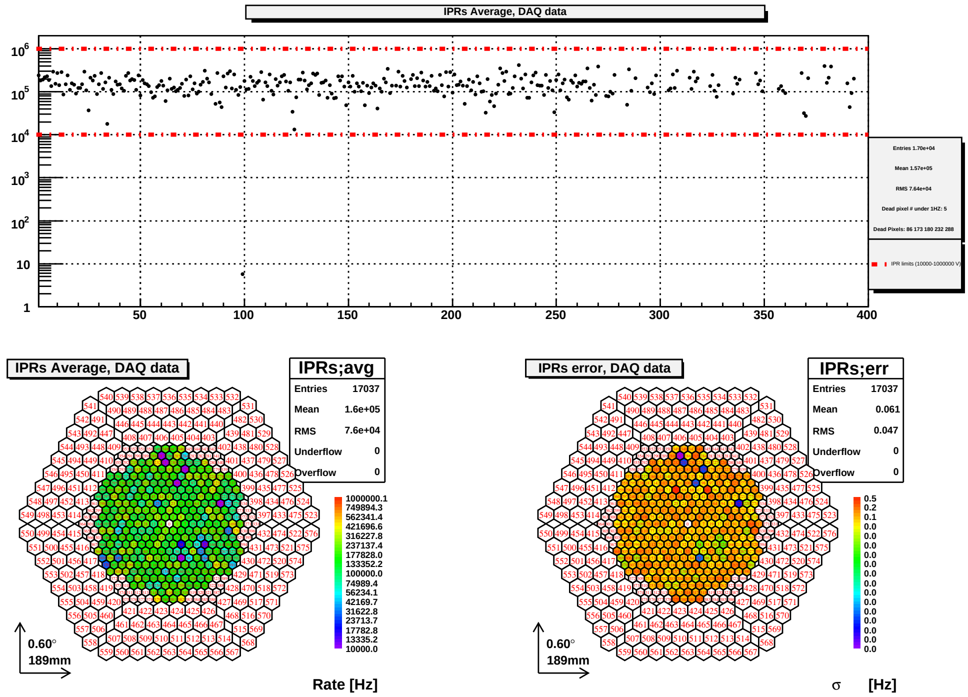

Figure 13: *IPR report plots. Top: time average of the IPR (Hz) versus pixel number. Red dashed lines show the limits of acceptable values of the IPR. The legend shows the number of the dead pixels, that are not plotted in the graph. Bottom: (left) time average of the IPR (Hz) in camera display and (right) time RMS of the IPR (Hz) shown as camera display.*

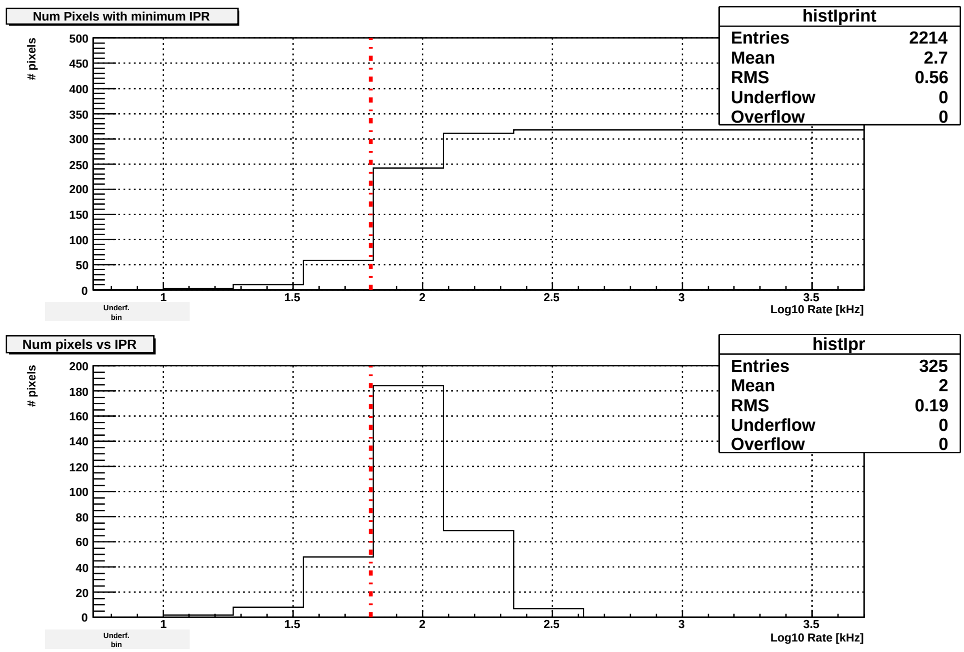

Figure 14: *More IPR report plots. Top: Number of pixels showing a minimum IPR (kHz). Bottom: Number of pixels with a certain IPR (kHz). Red dotted line marks the 60 kHz limit.*

Starguider This subsystem improves the pointing accuracy of the telescope. Its reports will indicate whether the telescope is pointing properly and will be important in the data analysis. The mispointing is determined by a comparison of the position of bright stars in a region of sky around the telescope pointing position and reference LEDs on the camera.

To check the telescope pointing stability, figure 15 displays the zenithal and azimuthal mispointing and the X and Y coordinates of the pixel in the CCD where the camera center is found versus time. Figure 16 the number of correlated stars and the sky brightness measured with the CCD camera versus time. A low number of recognized stars reduces the precision of the mispointing measurement.

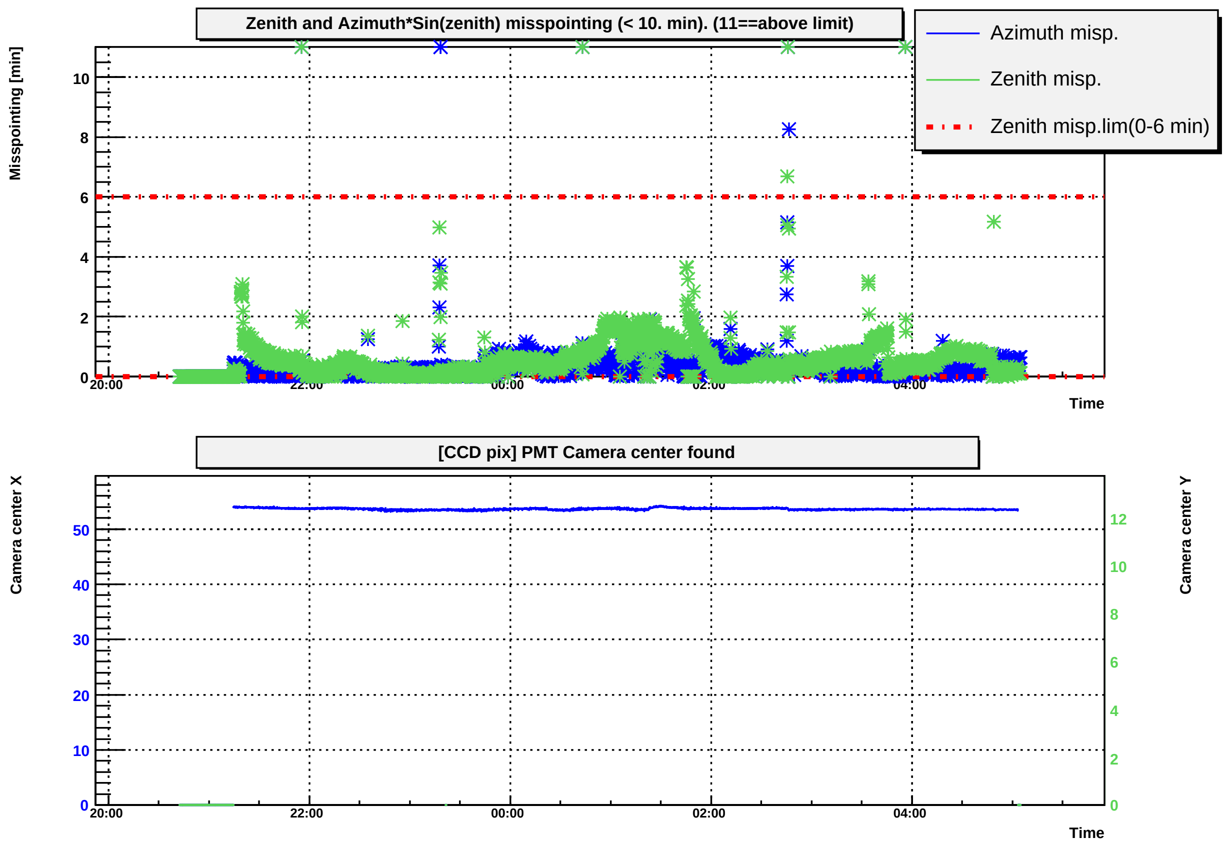

Figure 15: *Star guider report plots. Top: Absolute value of the zenith and azimuth mispointing (arcmin.) versus time. Bottom: The X and Y position in the CCD camera of the PMT camera center versus time. The red-dotted line corresponds to a mispointing within 1 camera pixel.*

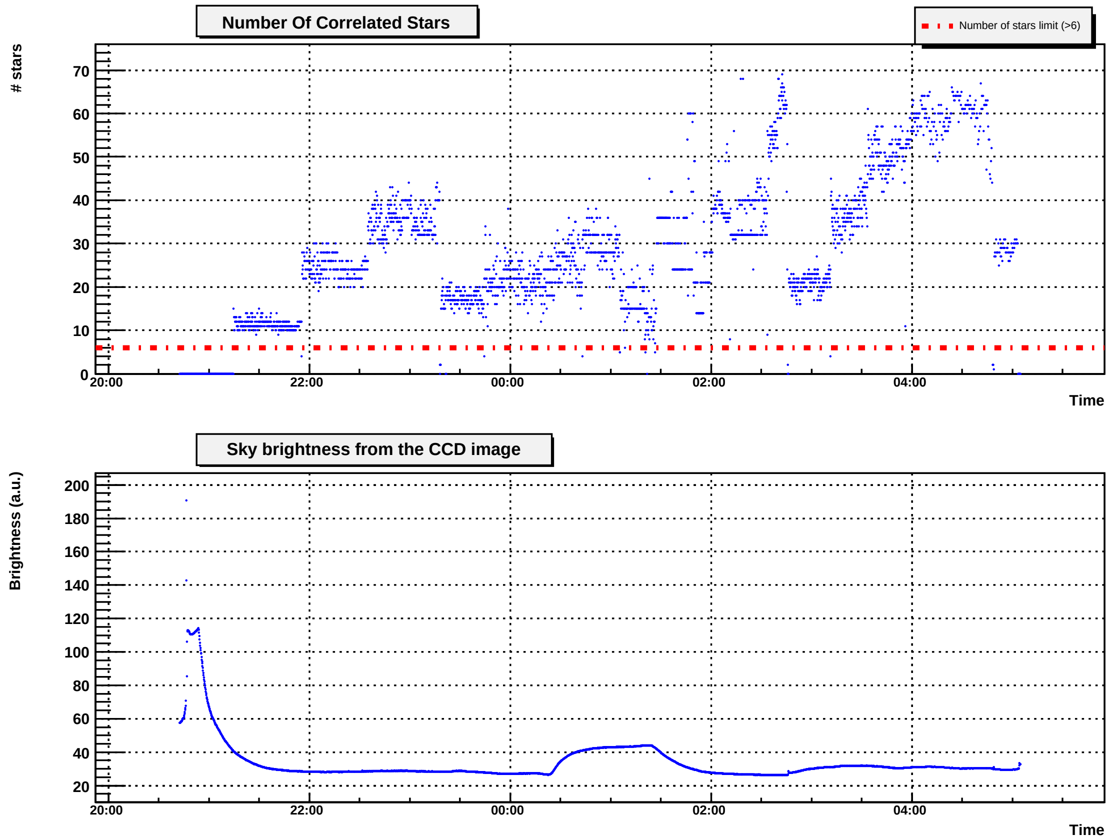

Figure 16: *Star guider report plots. Top: Evolution of number of stars correctly identified at the catalog. Bottom: Sky brightness (in arbitrary units) from the CCD image versus time. The red-dotted line corresponds to the minimum number of correlated stars found by the star guider system which is needed to compute a good mispointing estimate.*

Weather station The MAGIC telescope has its own weather station, located in the experiment vicinity. The values registered by the station are read out every 40 seconds and sent to a graphical display over the web, in different time scales. This web page can be accessed publicly [18]. As the other subsystems, the weather station also sends a report to the central control with all the gathered information.

The weather could affect the data quality but also to the telescope own integrity, since MAGIC is not protected by any dome. To check the weather conditions outside, the telescope data check program plots the humidity, the temperature and wind speed against the time (figure 17), together with its corresponding safety limits of operation.

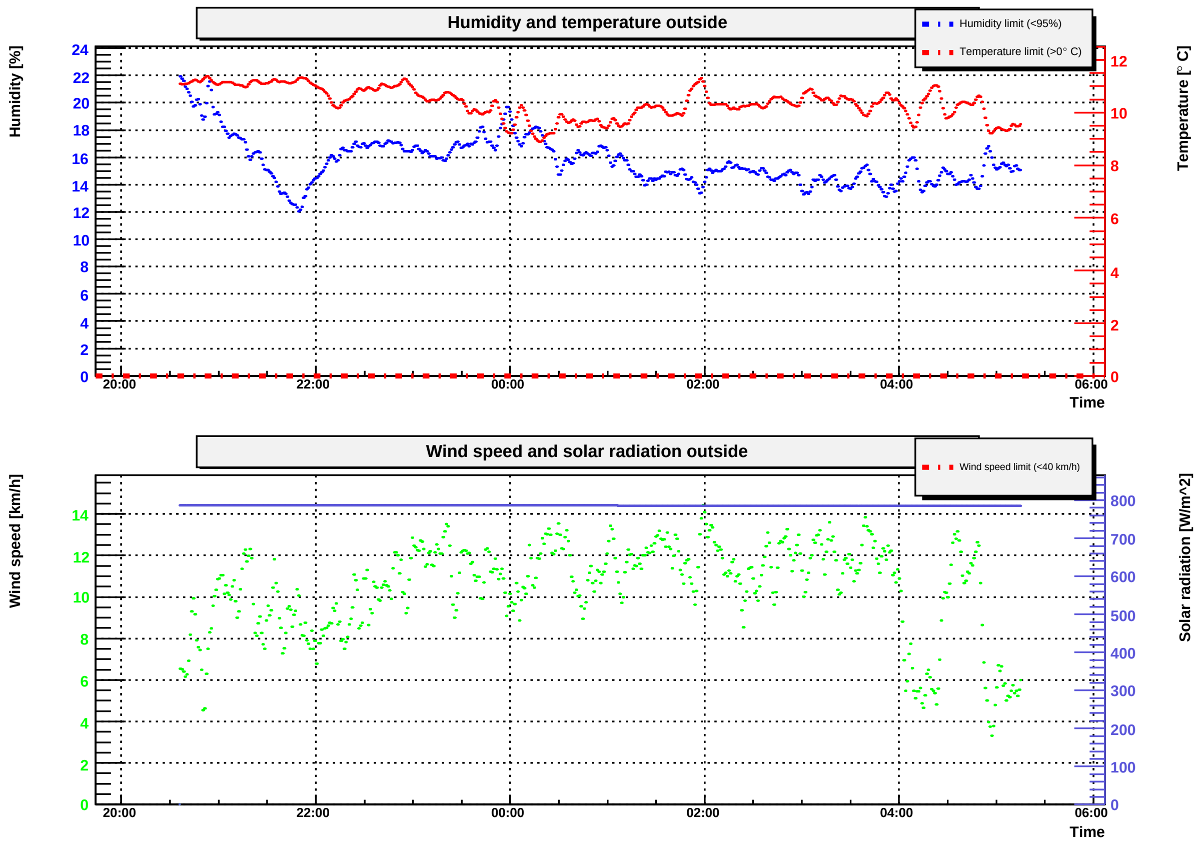

Figure 17: *Weather station report plots. On top: Humidity (blue) and temperature (red) outside versus time. On bottom: Wind speed (green) and solar radiation (violet) (not working in this example) versus time. The dotted lines correspond to upper limits for a safe telescope operation. Above these values it is advisable to park the telescope.*

Time The date and time information of a triggered event is determined on an absolute time scale, UTC and added to the data in the DAQ readout process. The time accuracy is achieved with a calibrated atomic clock (Rubidium clock), a MAGIC specific module called TIC (Time Interval Counter), a HM8125 GPS Time/Frequency Standard and sub-sec NIM modules. The Rub-clock is extremely stable at short time scales of minutes to days but drifts at longer time scales. In order to keep the atomic clock accurate, the drift is corrected by a reference time that remains accurate over periods of months and years. This is achieved by a radio receiver that synchronizes the rubidium time to GPS time. The time difference must be always within 1.2-1.75 μs. In case of a larger difference the GPS-Rubclock must be synchronized manually. A time difference higher than the limits may indicate that there is a problem with the GPS receiver, in the rubidium clock, or at the electronics that take care of the synchronization. Figure 18 shows the evolution of this difference.

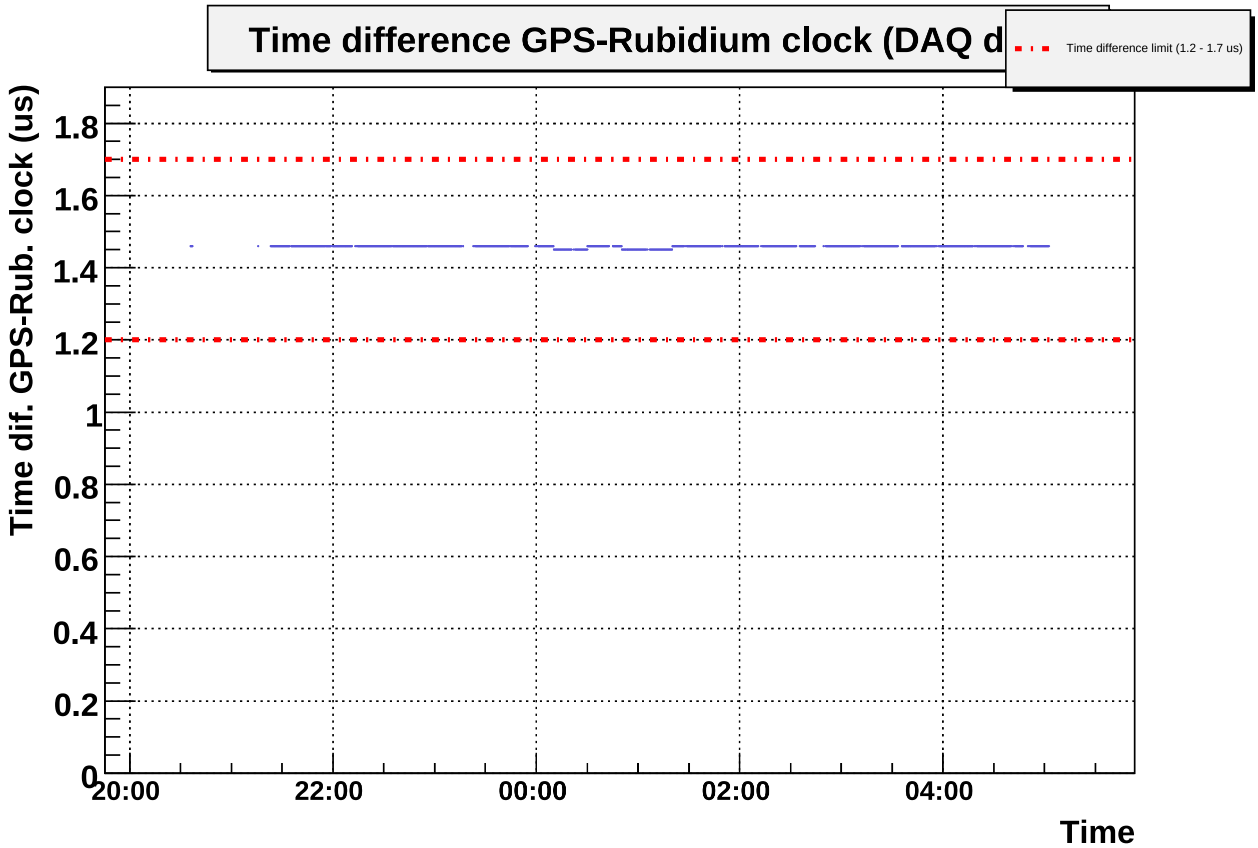

Figure 18: *Time report plot. Time difference (μs) between GPS and rubidium clock. The red-dotted lines are upper and lower limits.*

Receivers temperature Too high temperature at the receivers rack may affect the telescope performance. Moreover, fast changes of their temperature can provoke fast changes of the pedestal, calibration charges and signal charges. Figure 19 shows the evolution of the median of all receiver temperatures along the night.

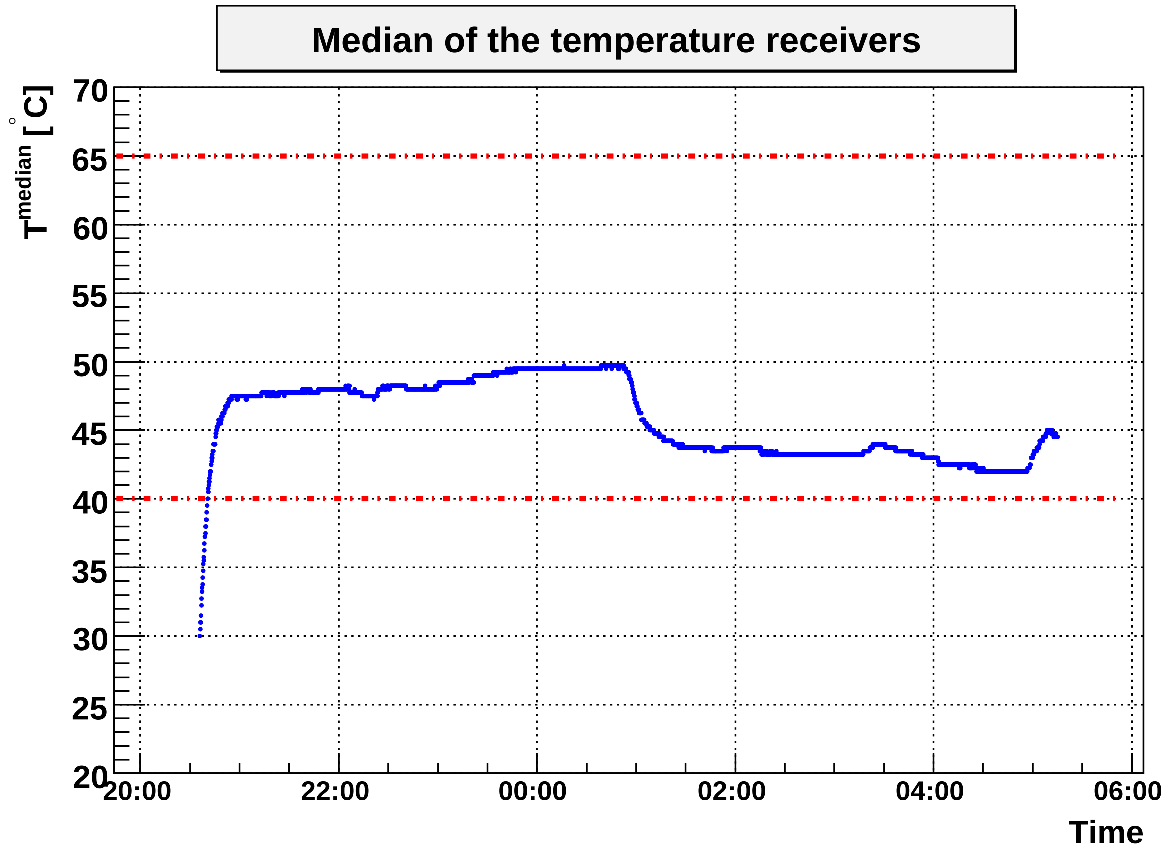

Figure 19: *Receiver temperature evolution along the night. The red dashed lines represent the safety limits.*

Trigger delays The function of the trigger delays is to compensate both the slightly different length of the optical cables and the transit time differences in the different PMTs due to construction and operation voltage differences. The trigger delays settings, fixed by experts, are saved to non-volatile memories in the receiver boards. It may happen that these memories get deleted, for example, after a power cut. The figure 20 allows to check if these delays are properly set.

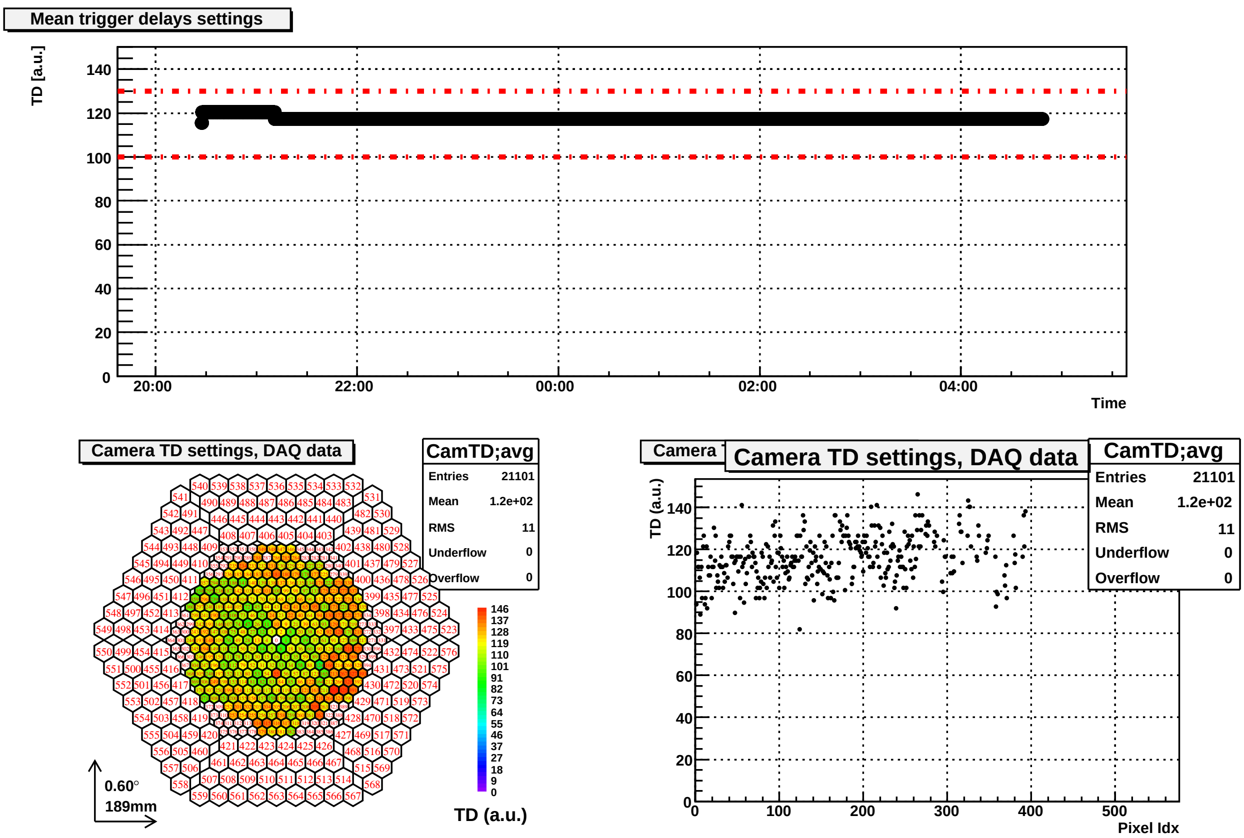

Figure 20: *Trigger delays. Top: Mean trigger delay evolution along the night. The correct region where the mean delay should be is defined by the red dashed lines. Bottom: Mean trigger delays of individual pixels for the whole data taking night.*

2.3 DAQ data check

The DAQ data check program processes the so-called DAQ statistics files of MAGIC-I. This program gives an overview on the status of the performance of the DAQ over the whole data taking night.

2.3.1 Overview

During the telescope data taking, the DAQ subsystem performs a simple analysis of the recorded events. This analysis determines an average pedestal, signal charge and arrival time for each event and pixel. The cosmics events are the ones that have given trigger. From these cosmic events, a pulse is defined as "signal" if it exceeds a certain FADC count value. Therefore, the collection of pixels whose charges exceed this threshold for a certain event constitute a cosmic "signal" event. For each data file, the threshold is defined in the DAQ statistics file, being 8000 FADC counts the default value for MAGIC-I.

The average sub-run results obtained from the previously described analysis are written to an ASCII file (/mnt/raid1/muxdata/dcheck_<date>.txt) at the end of each sub-run [10]. The format of the input file is described in the reference [17].

2.3.2 program

The part of the MAGICDC program which checks these DAQ is called by the script *MUXDCChecking*. This script joins all the night DAQ statistics files and merpps the joint, naming it as file (MuxDataCheck_M1_<year>_<month>_<day>.root). Finally, it calls a root-macro, *CheckMux.C*, to read the previously created .root files and display the corresponding subsystems report plots.

The check plots of this part are of two kinds: *camera display views* and *variable versus run*. They show the overall behavior of the camera for different parameters, and the evolution of these parameters during the night.

The log file of *MUXDCChecking* job, named MUXDCChecking_<year>_<month>_<day>.out, is copied, together with the results of the process, into the directory
/remote/raid2/analysis/DataCheck/analysis/<year>_<month>/<year>_<month>_<day>
/CCDAQCHECK.

An additional task made by the DAQ job is to launch the script *MUXDCCheckingMonth*, that works in the same way as *MUXDCChecking* but using as input all the information gathered during the month of study. The results are stored into the directory
/remote/raid2/analysis/DataCheck/Data/analysis/<year>_<month>/CCDAQCHECK.

2.3.3 Plots

Pixel charge In order to check the distribution of mean charges over the camera, figure 21 shows camera display views containing the mean pixel content of different type of events for the data taking night. Calibration events from dedicated calibration runs, and interleaved calibration events have been processed independently. Cosmic and cosmic "signal" events charges are also displayed. Finally, the hit fraction of cosmics "signal" events in percentage is plotted. The hit fraction of a pixel during a sub-run is defined as the ratio of the number of times that the pixels has a cosmic pulse tagged as "signal" over the total of its cosmic events.

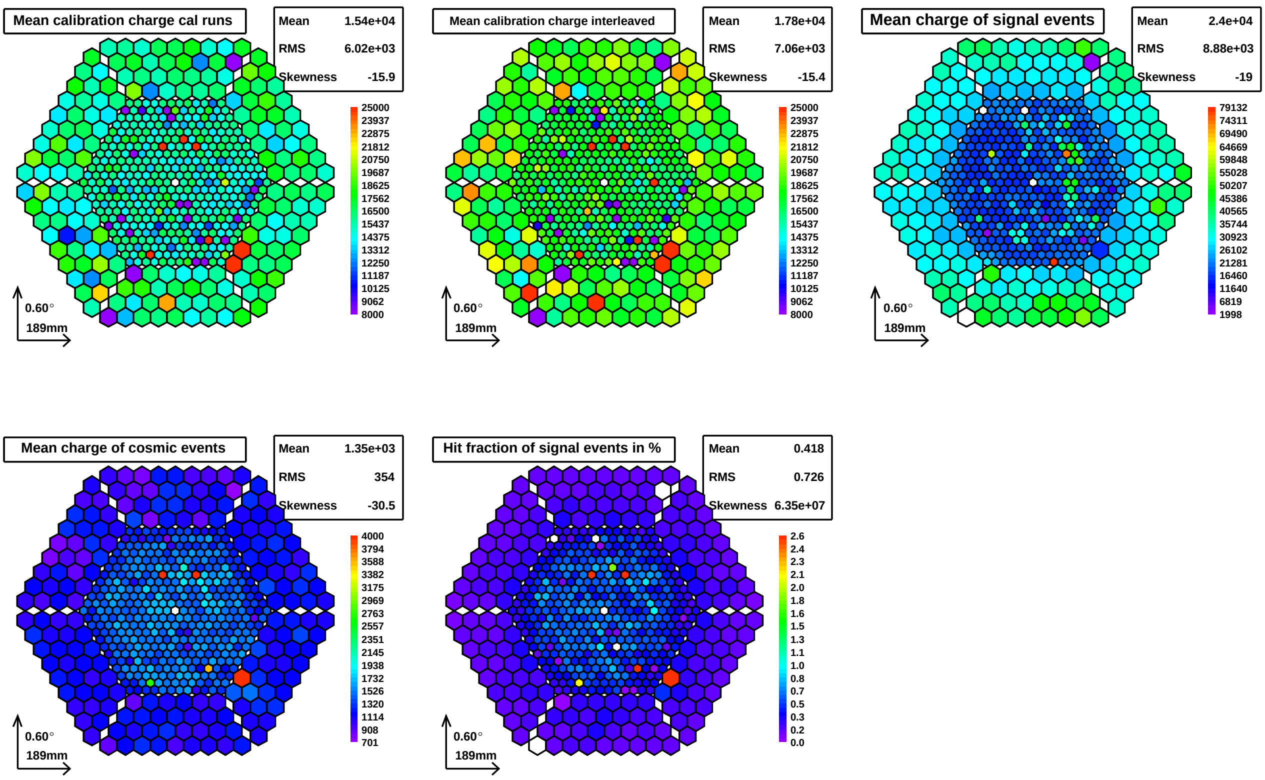

Figure 21: *Top left: Mean charge from calibration events of the calibration runs. Top middle: Mean charge the interleaved calibration events from data runs. Top right: cosmic signal events. Bottom left: The mean charge from cosmic events. For these events, all pixels are taken into account when a cosmics trigger occurred. Bottom middle: The hit fraction of cosmic signal events with respect to all cosmic events.*

Pixel time To check the distribution of the arrival times over the camera, figure 22 shows a camera display views containing the mean pixel value and RMS of this parameter for signal cosmic events and calibration pulses for the whole night. Again, calibration events from calibration runs runs and interleaved calibration events from dat runs have been processed and displayed independently.

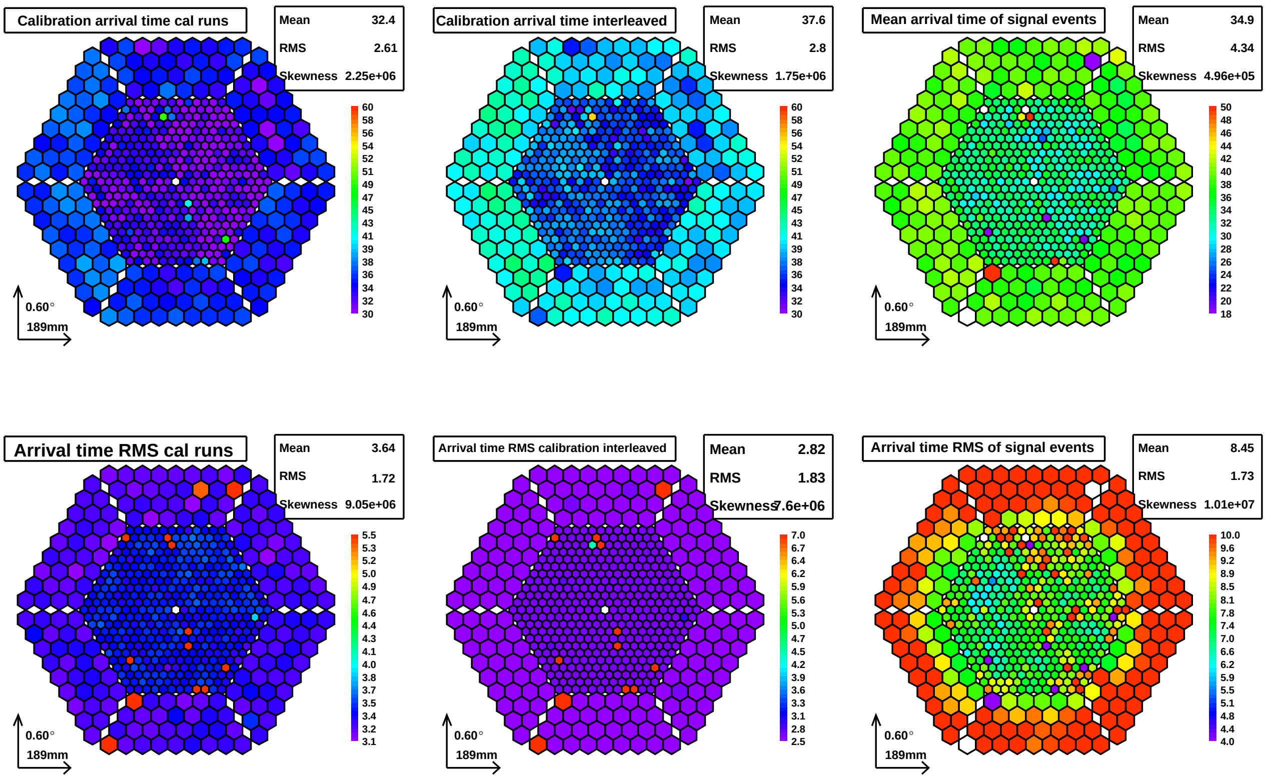

Figure 22: *Top left: Mean arrival time from calibration events of calibration runs. Top center: Mean arrival time from calibration interleaved events. Top right cosmic signal events. Bottom left: The arrival time RMS from events of calibration runs. Bottom center: Arrival time RMS from calibration interleaved events. Bottom left: Arrival time RMS from cosmic signal events.*

Pixel pedestal The distribution of pedestals over the camera can be checked at figure 23. It shows camera display views containing the mean pixel value and RMS of the pedestal in FADC counts for both pedestal and data runs for the whole night. The value of pedestal RMS is obtained as RMS from the number of slices of the pedestal extractor window divided by the number of slices. The number of photo-electrons and the conversion factor from FADC count to photo-electrons are also shown at figure 23. To calculate the number of photo-electrons, the excess noise factor was used, through the formula:

$$Npe = F^2 \frac{< Q_{cal} >^2}{\sigma^2_{calQ} - \sigma^2_{ped}}, \; with\, F^2 = (1.15)^2 \tag{1}$$

To apply the previous formula, one has to take into account that in the input DAQ statistics file the pedestal RMS is obtained for a certain pedestal extractor size, different from the signal extractor window size. In the actual MAGIC-I configuration, 50 slices for the pedestal extractor and 10 slices for the signal extractor are used, whereas 40 and 7 slices respectively are used for the MAGIC-II configuration. For MAGIC-II F has not been calculated yet, but it is estimated as $F^2 \leq 1.1$.

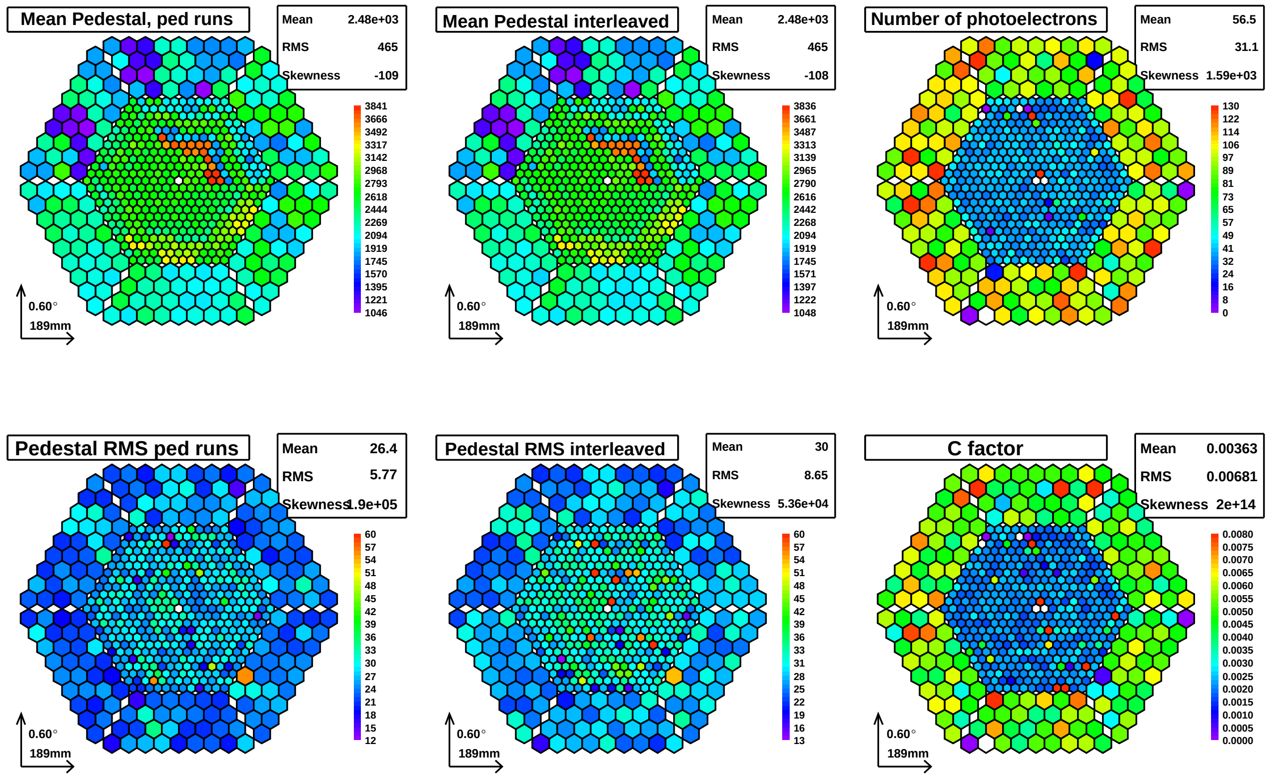

Figure 23: *Top left: Mean pedestal from events of pedestal runs. Top center: Mean pedestal from interleaved events. Top right: Number of photo electrons from interleaved calibration events . Bottom left and center: Pedestal RMS from events of pedestal and data runs. Bottom left: Mean conversion factor from FADC counts to photo-electrons.*

Charge and Pedestal evolution Figure 24 shows the evolution along the night of the median value of the charge for calibration and cosmic signal events. Inner and outer camera are treated separately. It also shows the evolution of the median pedestal and its RMS for both inner and outer camera.

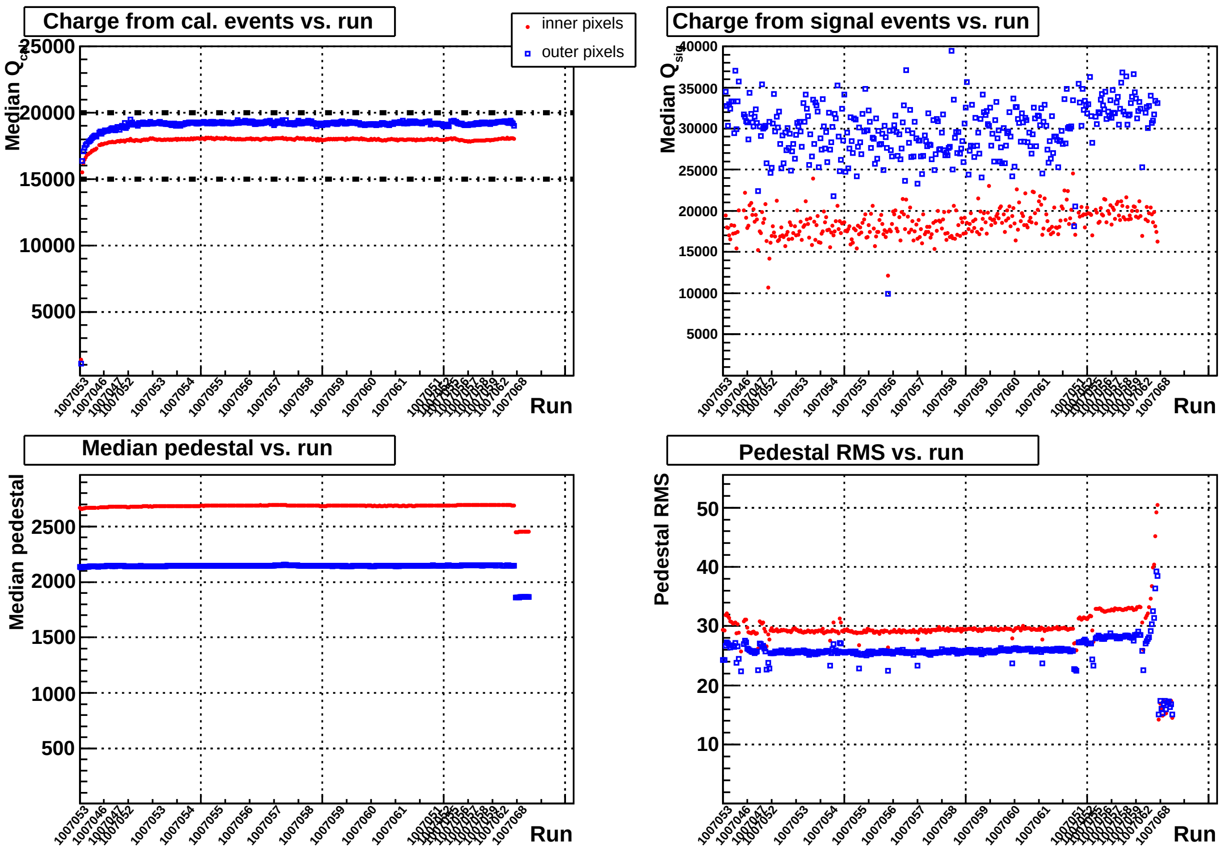

Figure 24: *Top: Evolution of the median charge for calibration (left) and cosmic signal events (right) versus run number, for both inner and outer pixels. Bottom: Average pedestal and its RMS for inner and outer pixels.*

Arrival times evolution Figure 25 shows the evolution along the night of the median and RMS value of the arrival time, in units of FADC slices, for calibration and cosmic signal events. Inner and outer pixels are treated separately.

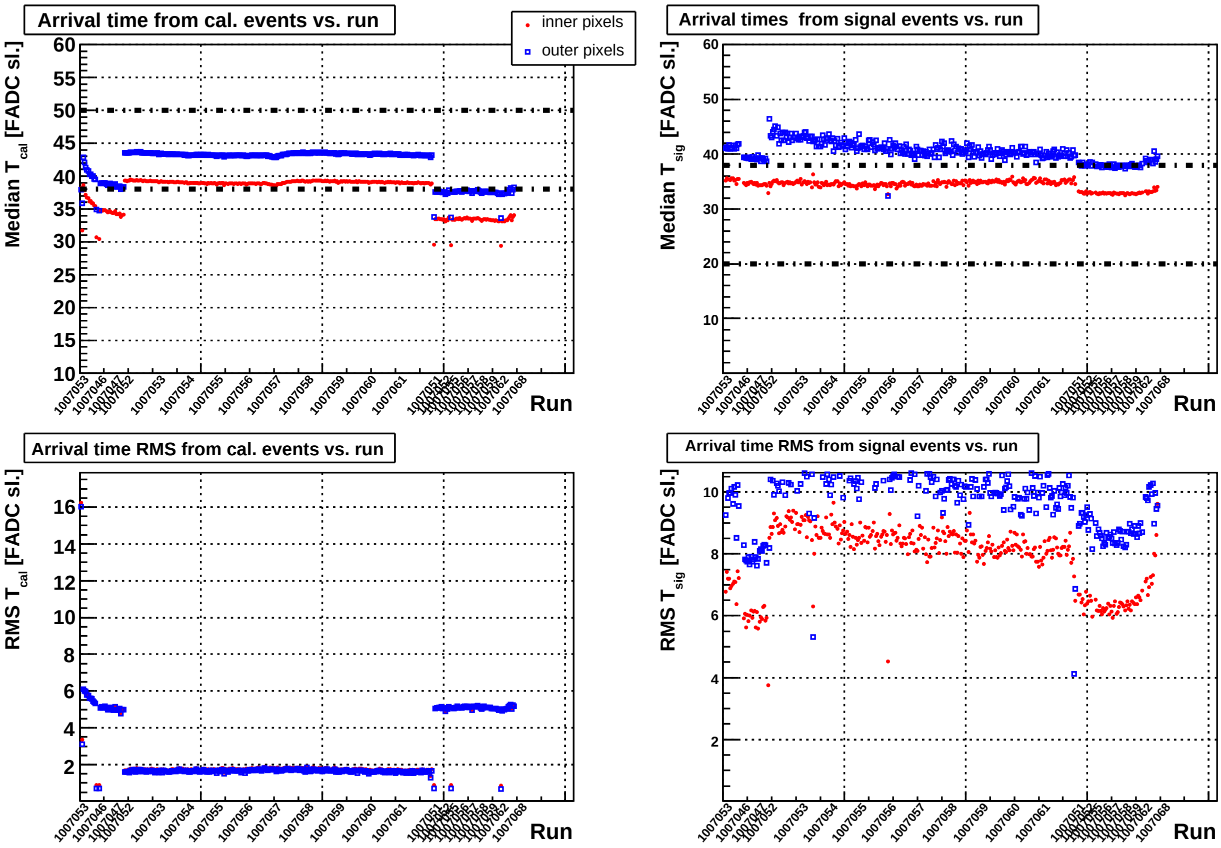

Figure 25: *Top: evolution of the arrival times for calibration (left) and cosmic signal events (right), for both inner and outer pixels. Bottom: RMS of the arrival times for calibration (left) and cosmic signal events (right), for both inner and outer pixels.*

Calibration factors evolution Figure 26 shows the evolution over the night of four different parameters. The first plot shows the evolution of the number of photo electrons calculated according to formula (1), for inner and outer pixels. For representation reason, the outer pixels Npe is scaled by a 0.4 factor. The second plot shows the average conversion factor form charge to Npe for both types of pixels, again scaled by a factor 0.4 for outer pixels. The third plot shows the evolution of the hit fraction of events in percentage of cosmic signal events over the total cosmics events. The last plot shows the evolution of the average ratio of charge in cosmic events to the pedestal RMS for both inner and outer pixels.

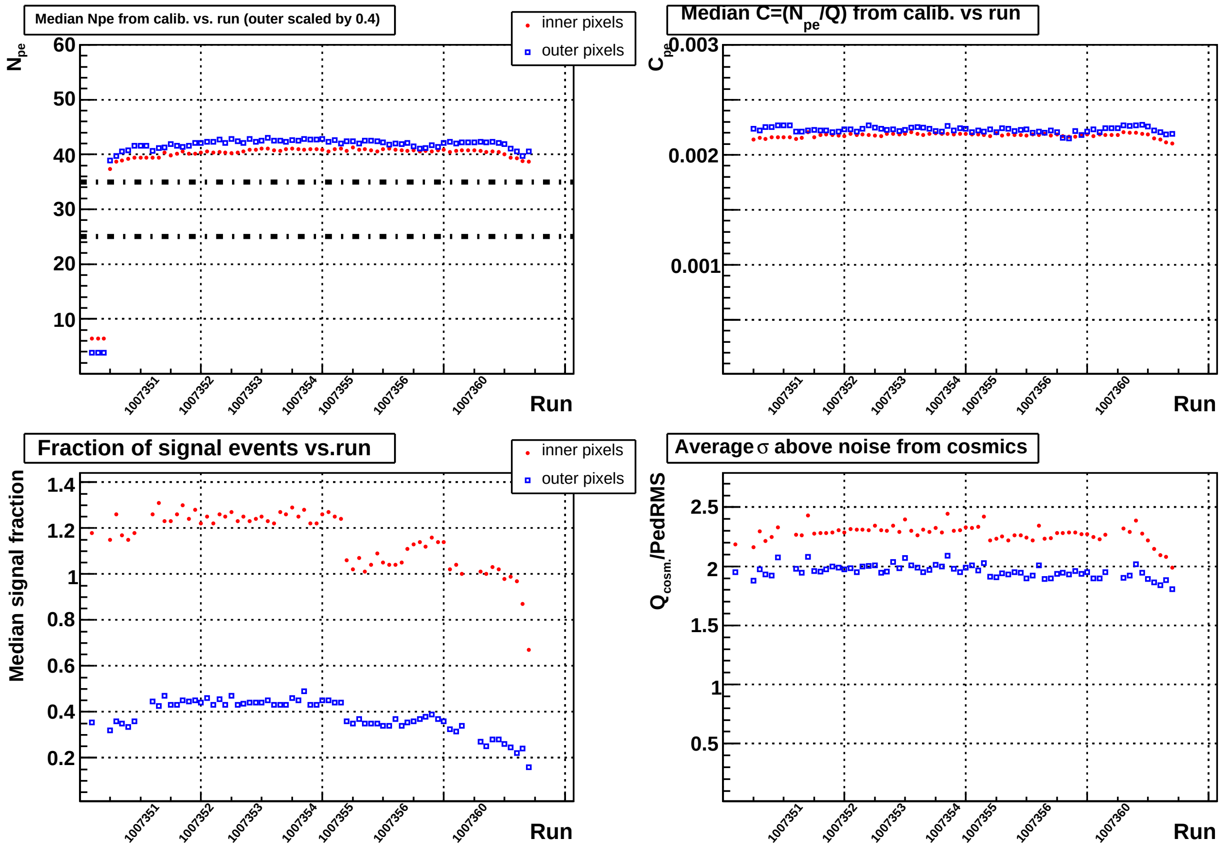

Figure 26: *Top left: Evolution plot of the Npe along the night for interleaved calibration events. outer pixels numbers have been scaled a 0.4 factor. Top right: median conversion factor from FADC counts to photo electrons from interleaved calibration events for inner and outer pixels. Bottom left: hit fraction of cosmic signal events. Bottom right: averaged ratio of charge in cosmic events to the pedestal RMS*

Arrival time differences The top panel of figure 30 shows the maximum difference of the average arrival time in FADC slices of any two pixels, for different type of events, in terms of the data run, calculated separately for inner and outer pixels. Bottom left panel shows the evolution of the averaged difference between arrival times of calibration and signal events, obtained as the difference between the median arrival time of calibration events and the median arrival time of cosmic "signal" events. The bottom left panel of figure 30 shows the difference of arrival times for calibration and cosmic "signal" events between two particular pixels: 173 and 197. The positions of these two pixels in the camera are located approximately at half distance between the camera center and the camera edge, symmetrically with respect to the camera center.

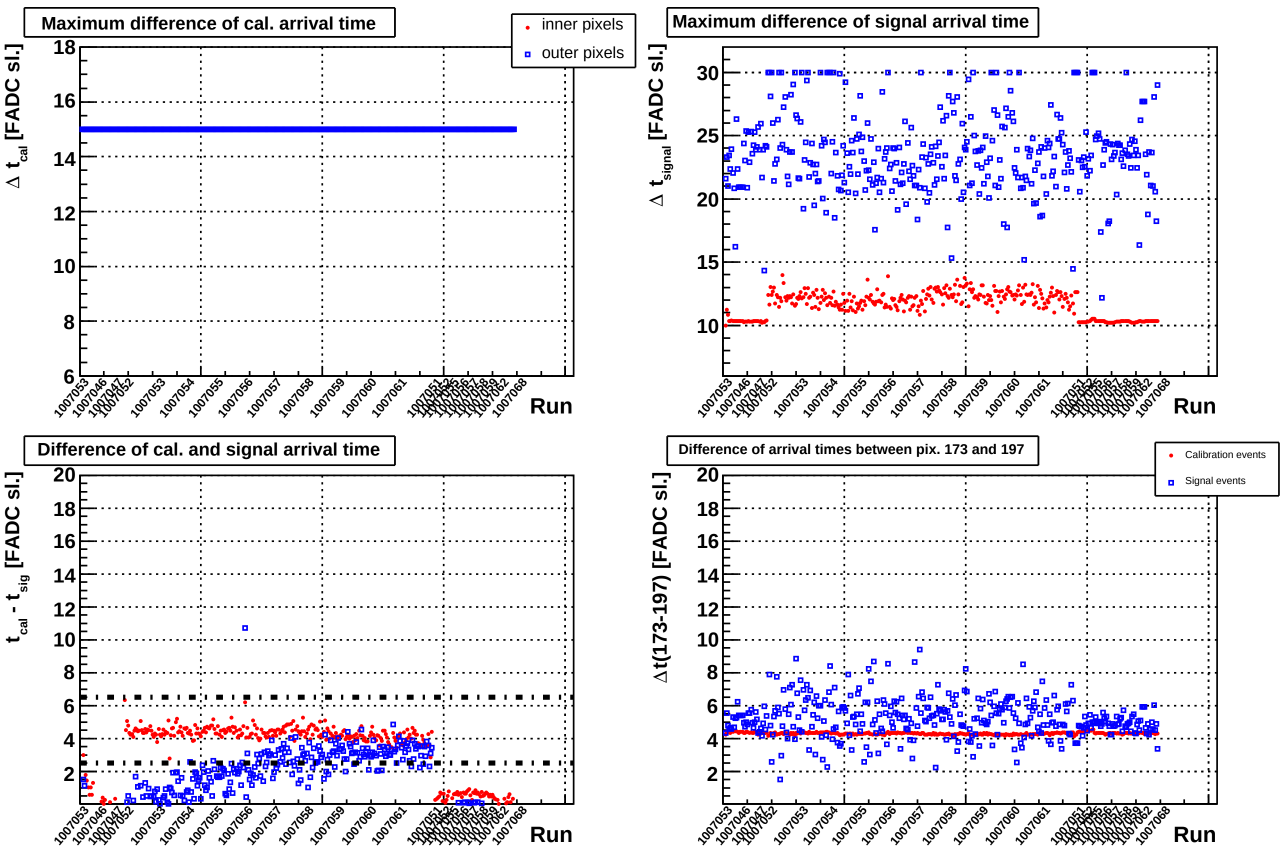

Figure 27: *Top left: maximum arrival times difference between pixels for calibration events. Top right: Maximum arrival time differences between two pixels for cosmic signal events. Bottom left: average arrival time difference between calibration and cosmic signal events. Bottom right: Arrival time difference between pixels 173 and 197, for calibration and cosmic signal events.*

Arrival time check The arrival times at the FADC should be correctly set in order to be sure that the pulses are never truncated. The best criterion to decide if these arrival times are correctly set has to take into account their mean and RMS. We have decided to impose a lower and upper limit on a combination of the mean and the RMS of the arrival times, according to the following rule:

$$\overline{T}_{cal} - 2\overline{\sigma}_{Tcal} > Lower\ limit, \tag{2}$$

$$\overline{T}_{cal} + 2\overline{\sigma}_{Tcal} < Upper\ limit, \tag{3}$$

The ideal limits would be 10 slices away from both lower and upper limits of the DAQ window, with additional 10 more slices in the upper limit to take into account the physical time evolution of the showers. The corresponding limits for MAGIC-I have to be modified to considering that from the total of 80 slices, the first 15 and the last 15 are affected by the switching noise. For MAGIC-II, from the total of 70 slices the first 20 are used to extract the pedestal baseline. In summary, this means that the lower limits are 20 for both telescopes, and the upper limits are 44 and 49 for first and second telescope respectively.

Figure 28 shows the evolution of the check of the arrival times for MAGIC-I telescope, for both inner and outer pixels.

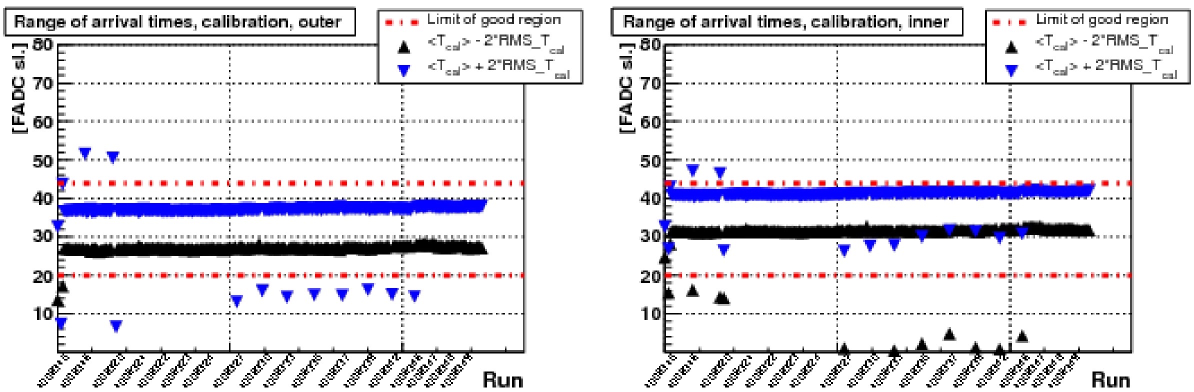

Figure 28: *Evolution of quality check test for arrival times of calibration pulses along the night.*

Bad pixels Figure 29 shows the evolution, in terms of the run number, of the number of the bad pixels present in the camera. A pixel is tagged as bad if it falls at any of these criteria:

- The calibration signal contained only pedestals and therefore is presumed that it is a dead pixel.
- The signal has its average maximum in the first used FADC slice. The signal comes so early in the FADC window that the pulse was not extracted correctly.
- The signal has its mean maximum in the last two used FADC slices. The signal comes so late that the pulse is not extracted correctly
- The calculated number of photo-electrons deviates by more than 6 standard deviations above or 5.5 standard deviations bellow the calculated mean number of photo-electrons of the same type of pixels. The reason of this behavior should be a malfunctioning of the channel or the extraction algorithm.
- The pedestal root mean square was at least 4.5 standard deviations below or 25 standard deviations above the average value obtained for its type of pixel. The lower limits looks for dead pixels, while higher limit looks for too noisy pixels, that show highly fluctuating gains.
- The arrival time for calibration pulses does not fulfill the conditions of formulae (2) and (3). For this pixel some of the pulses are truncated.
- The mean value of the charge from calibration of the pixel is below 0.5 times or above 1.5 times the mean value of the type of pixels. This means that the pixel is obviously very strongly mis-flatfielded. This effect occurs typically to "dying" PMTs, which can later on show strong gain variations, in this case the pixel should be discarded for the data analysis.

Following teh previous criteria, it is normal to have around 20-30 bad pixels in the camera.

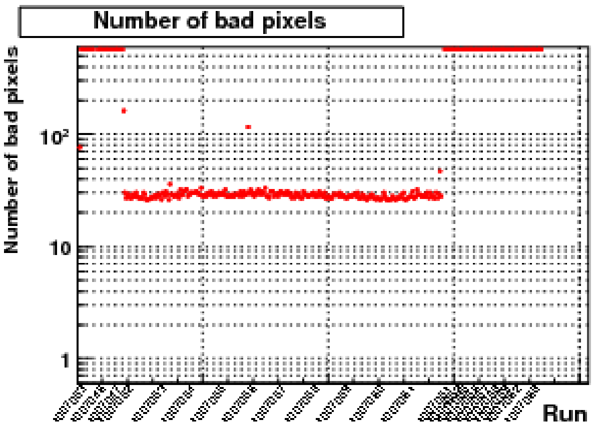

Figure 29: *Evolution of number of bad pixels over the data taking night.*

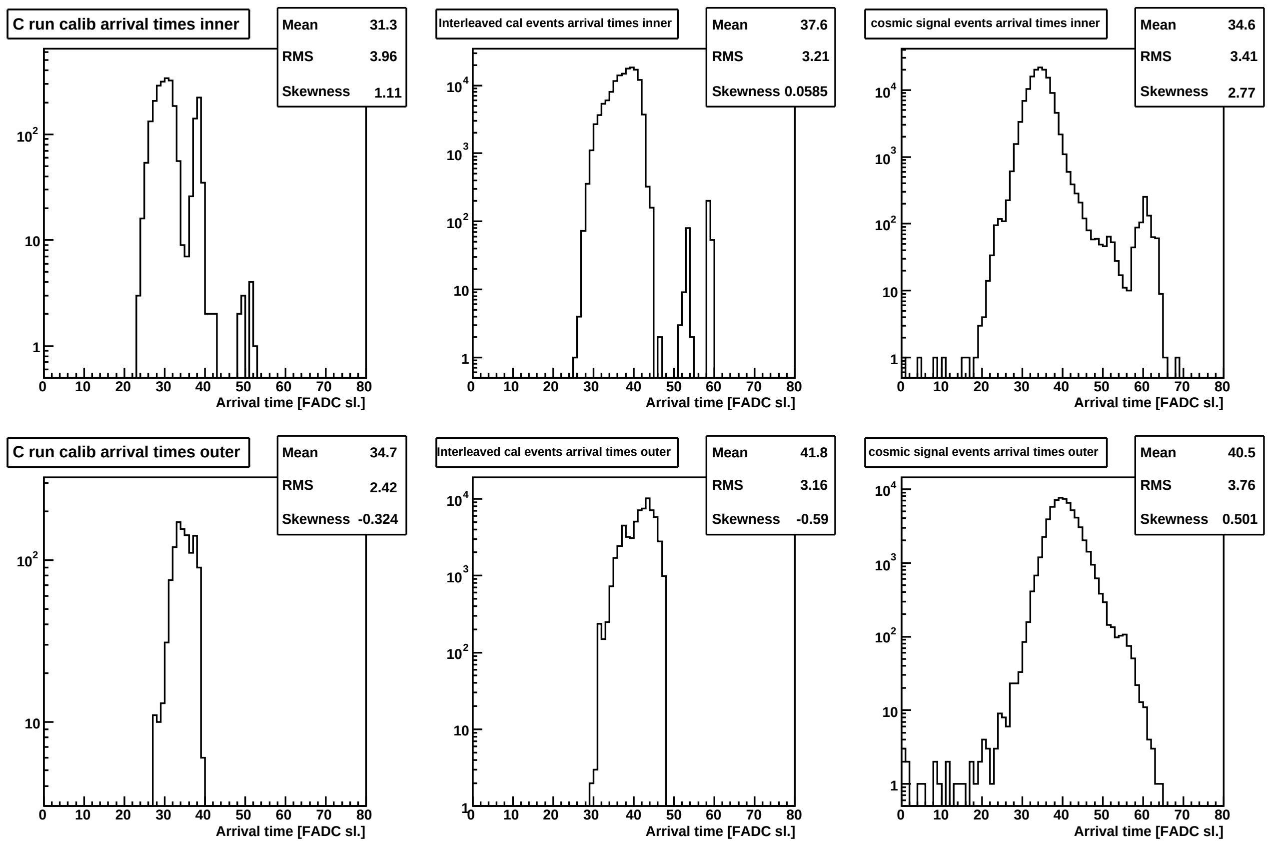

Figure 30: *Top, from left to right: Arrival time distribution of calibration pulses from calibration runs, calibration pulses from data runs and cosmic signal arrival times, for inner pixels. Bottom: same arrival distributions for outer pixels*

Arrival time distributions With the aim of checking if all pulses are arriving inside the window, and with the approximate same position, figure 30 shows the distributions of arrival times for calibration pulses and cosmic signals. The histogramd include the statistics for the whole night. For each run, the mean of the arrival time of each pixel is used to fill the histogram. The correct window for MAGIC-I is from slice 15 to slice 65, whereas from MAGIC-II it is from slice 20 to slice 60.

2.3.4 MAGIC-II update

In order to check the quality of the data taken during the commissioning phase of MAGIC-II, a modification of the macro *CheckMUX.C*, named *CheckDomino.C* has been created. It makes the same set of plots of the first macro, but with the information gathered by the MAGIC-II DAQ statistics file, that can be found at
(/mnt/raid4_1/M2rawdata/dcheck/DominoDataCheck_<date>.txt) The format of the input file is the same as the the one of MAGIC-I. For the time being the safety limits of the parameters have no been established yet and therefore this data check step is in a preliminary state.

2.4 Calibration data check

The calibration data check step performs a full determination of the calibration parameters using the previously mentioned standard collaboration software, MARS. At this step, we will check the response of the whole light detection and amplification chain to get the correspondence between the incident Cerenkov light and the digitazed information. This is done through the data calibration process which determines the conversion factor between digitized FADC counts and incident photons, and the arrival time delay for each pixel. More information can be found in [9].

2.4.1 The calibration system

The MAGIC telescope requires a precise and regular calibration system of the camera and the readout chain over a large dynamic range of amplitudes. This is achieved with the help of a number of powerful ultra-fast LED pulsers located inside a pulser box. A pulsating mode (pulser box) is used to calibrate the detector response to Cerenkov light with 2 ns pulses, while a continuous mode is used to calibrate the response of the DC readout to background light (star and moonlight). The absolute light flux is calibrated using three blind pixels hosted at the camera and a calibrated PIN diode located at 1.1 m distance from the pulser box [9].

For the calibration process two kind of runs are taken consecutively: the first one is a pedestal run, which consists of 1000 events triggered by a random signal sent by the calibration box to L2T. These events should contain nearly no Cerenkov pulses. The second one is a calibration run, which contains 4096 events of light pulses sent by the calibration box following a number of actions predefined by a calibration script.

In a first stage, the MAGIC camera itself was used to measure the absolute amount of photons emitted by the light pulser and calibrate the data, using the so-called “F-Factor” method. But the results of this method change with the unknown ageing of the PMTs. For this reason two more methods are now used to calibrate the individual camera pixels with respect to the amount of photons produced in each calibration light pulse, they are the so-called “blind pixel” and “PIN-diode” methods.

Several signal reconstruction algorithms have been studied to extract the charge and arrival time from the calibration and data runs with the highest resolution and minimum effect of the noise [9][3]. For some time the most used extractor algorithm for low energies and timing information was the so-called “Digital Filter”[2]. Later on, the spline extractor was set as default being the actual extractor used in MARS and therefore in the data check program [9][3] .

2.4.2 Program

The script which carries out the calibration data check is named *DAQDataChecking* (fig. 1) and is called through option “cal” on *launcher* main script. It consists of three logical parts:

I. The first task of the *DAQDataChecking* script is to define the callisto-sequences (sec. 1.2). To do this the script reads the central control .run files (joined in CC_<year>_<month>_<day>.run file) which contains a summary of the night data taking. Then a night summary file (NightSummary_<year>_<month>_<day>.txt) is created with the variables needed by the program. From this night summary file thr run information is extracted to build the analysis sequences.

   As it has been explained before, to extract and check the calibration constants it is necessary to have a pedestal-calibration pair of runs. With each of these pairs we define a sequence for the *callisto* MARS executable.

   Then *callisto* is run on the sequence, it calculates the calibration parameters and saves them into a "calib<SequenceNumber>.root" file. This file is then read by the MARS executable *showplot* making the calibration data check plots (see next section for a description) and saving them as a PDF file.

   Finally, for each sequence the *RunDAQDC.C* macro is run and saves all the sequence information from pixel calibration into an ASCII file, named as "BadCalPixels_<Source>_<PedestalRun>_<CalibrationRun>.dat".

II. The second step is to run a set of macros to perform several other checks over all the night calibration constants already calculated (calib.root files of all sequences):

   - *NightDAQDC.C*: Plots the calibration parameters evolution versus time. It can be used to see the evolution of these values over the whole night [21]. The plots are stored in the file named as "AllNightDataCheck_<year>_<month>_<day>.pdf".
   - *AnalysisSample.C*: Creates an ASCII file called "samples.txt" with all the information of the night sequences. It will be used in the analysis data check (see . [15]).
   - *get_timediff_pcrub.C*: Calculates the time difference between the PC and the Rubidium clock for the first events each calibration and pedestal run. The results are displayed in a Postscript file named "TimeDiff_<year>_<month>_<day>.pdf" and in an ASCII file named "TimeSummary_<year>_<month>_<day>.dat".
   - *GetAtimes.C*. Obtains the arrival time distributions of the calib.root and signal.root from the on-site analysis output [15]. The macro is called by the on-site analysis script *sequencer.csh*. This script also converts the output file to .PDF format. Results are available at same directory of calibration data check results, named as Atimes_MARS_<year>-<month><day>.pdf

   All the mentioned Postscript files are converted to Portable Document Format (.pdf) files and saved all together at /mnt/raid1/analysis/DataCheck/Data/daqdata/<year>_<month>/<year>_<month>_<day>/, where the job log file CALDataChecking<year>_<month>_<day>.out.

III. The last set of macros (see fig. 1) corresponds to the manipulation of a ntuple which accumulates and stores relevant information about the calibration (*MakeTreeDAQ.C* macro) and then it is plotted (*ReadTreeDAQ.C* macro) into a Postscript file named "DAQCntuple.ps". These last result plots are saved into this directory /mnt/raid2/analysis/DataCheck/Data/ [21].

2.4.3 Plots

Switching noise peak position Figure 32 is a camera display where the mean switching noise position for each pixel of the sequence is shown .

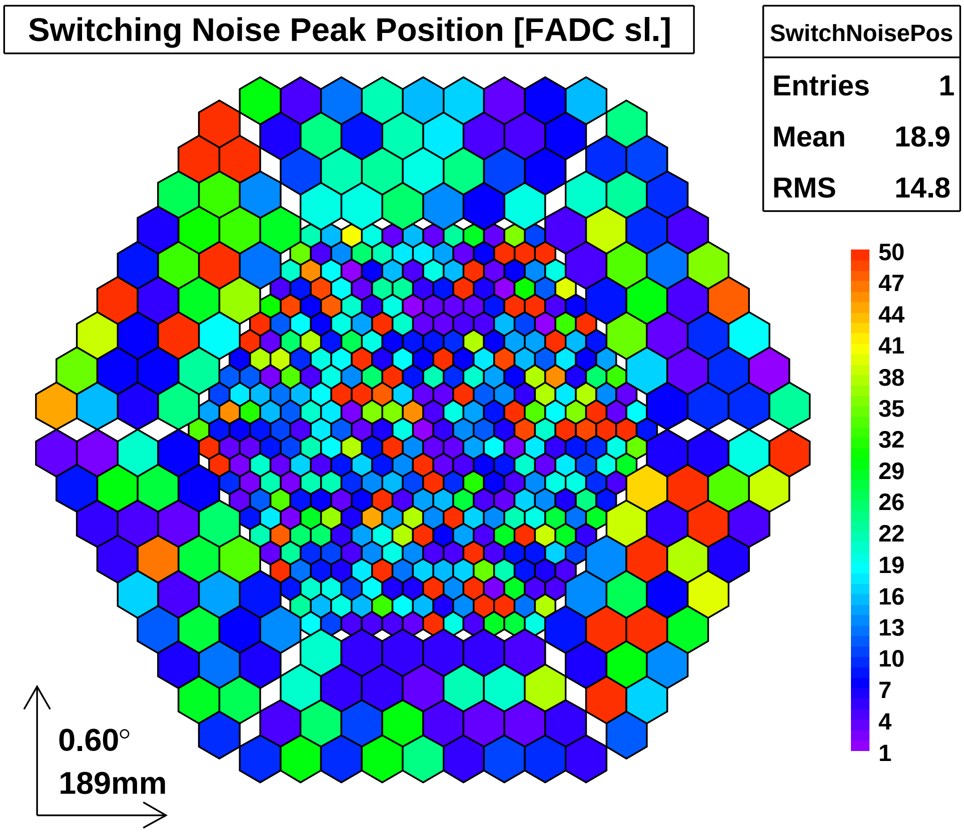

Figure 31: *Camera display containing each pixel's switching noise peak position in units of FADS slice.*

Pedestals from pedestal run Figure 32 displays the mean and RMS of the pedestal charge distribution for each pixel versus the pixel index as a profile and as a camera display, and also their distributions. The mean and RMS camera distributions are fitted to gaussians. In the case of the RMS there are two plots, corresponding to the inner and outer part of the camera (or pixels) and the text shows the integrated number of pixels -4.5σ away from the distribution mean mean, that are the so called "dead" pixels and those at +25σ, that are the "noisy" pixels.

The reference lines correspond to the values "RefPed{ClosedLids/ExtraGalactic/Galactic}" and "RefPedRms{ClosedLids/ExtraGalactic/Galactic}{Inner/Outer}" specified in the .rc file MJPedestalC1.ReferenceFile of "callisto.rc".

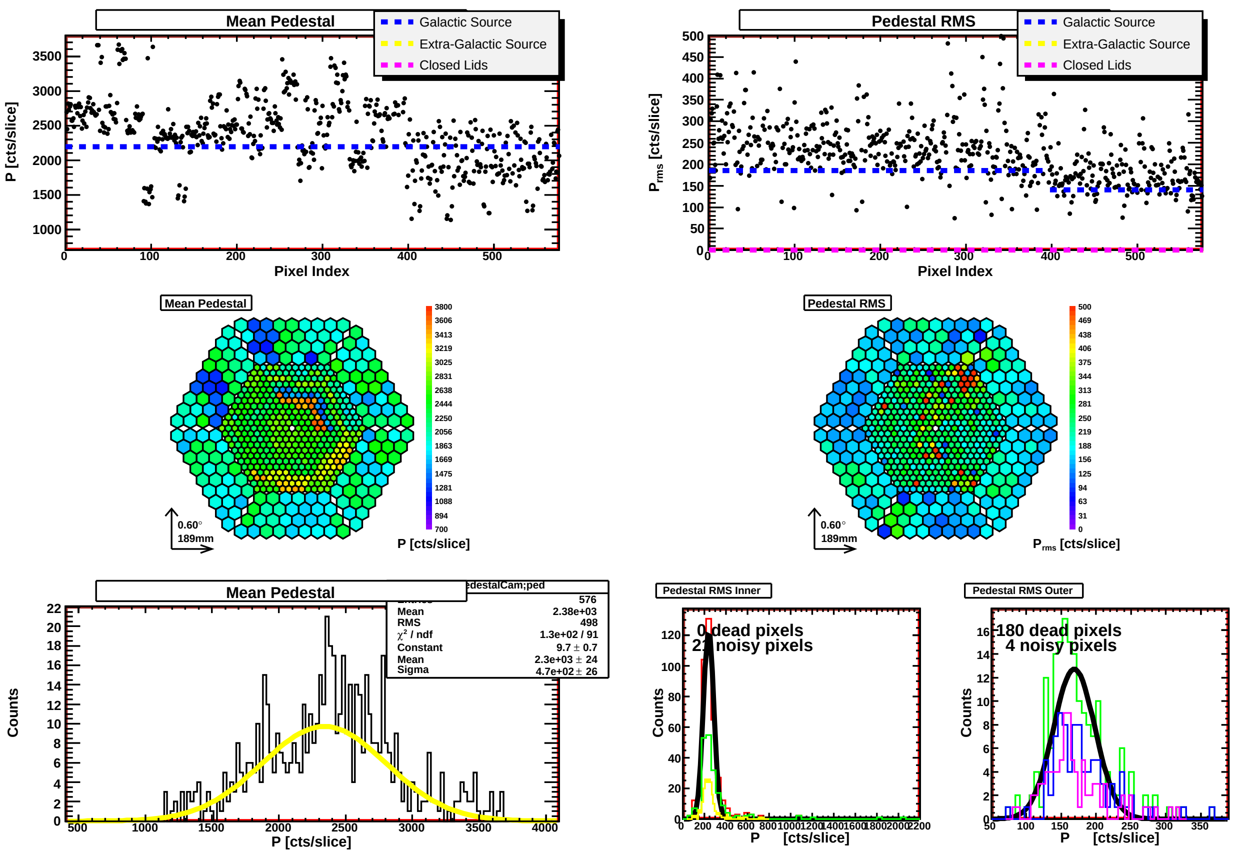

Figure 32: *Pedestal mean and RMS (from pedestal run). From top to bottom: pedestal mean (left) and RMS (right) versus pixel index viewed as a profile and camera display views, and the mean and RMS distributions together with the Gaussian fits. The reference lines correspond to the typical pedestal values obtained pointing to galactic (blue) or extragalactic (yellow) sources and with closed lids (pink).*

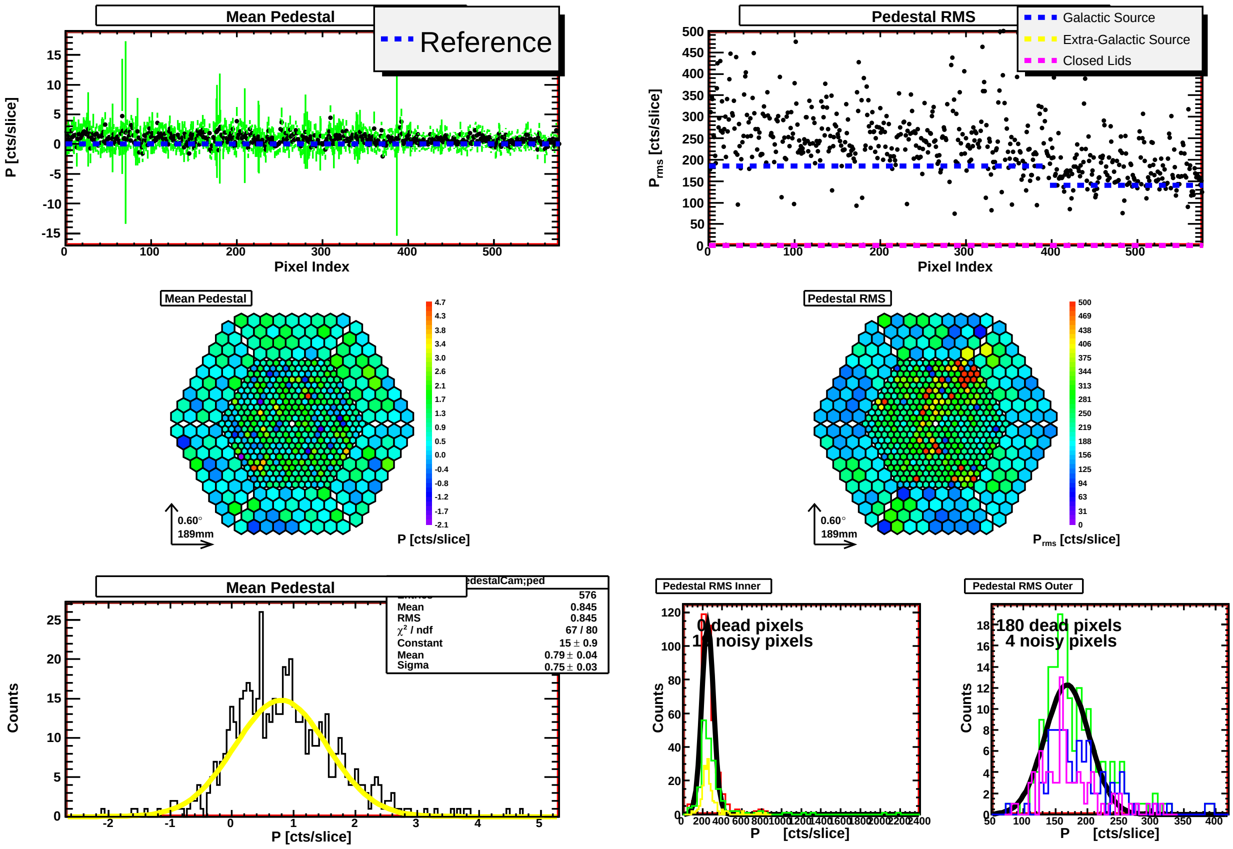

Figure 33: *Pedestal Mean and RMS (from calibration extracted run). From top to bottom: pedestal mean (left) and RMS (right) versus pixel index in profile and camera display views, and the mean and RMS distributions together with the gaussian fits. The reference lines correspond to the pedestal values when pointing to galactic (blue) and extragalactic (yellow) sources and with closed lids (pink).*

Pedestal from signal extractor The default extractor for MUX FADC data is the spline extractor [2]. The extraction region is from the slice 15 to slice 65. . The extracted pedestal is updated every 500 of these "pedestal events". As in figure 32, figure 33 display views the mean and RMS of the pedestal charge distribution but from the calibration extracted signal, where the pedestal has already been subtracted. Therefore the plots are similar to those in figure 32 but in this case the mean pedestal is expected to be 0 (blue reference line) for all pixels and the camera pedestal distribution should be centered at 0.

Arrival time Figure 34 represents the distribution of mean arrival times (FADC sl.) of the calibration signal events, as well as its behaviour versus time (sec). The plot is separated in inner and outer pixels. The position of the half maximum at the rising edge of the pulse determines the arrival time.

The reference line corresponds to the reference default values ("{Inner/Outer}RefTime") on .rc MJCalibration.ReferenceFile file of "callisto.rc" file of the MARS release version.

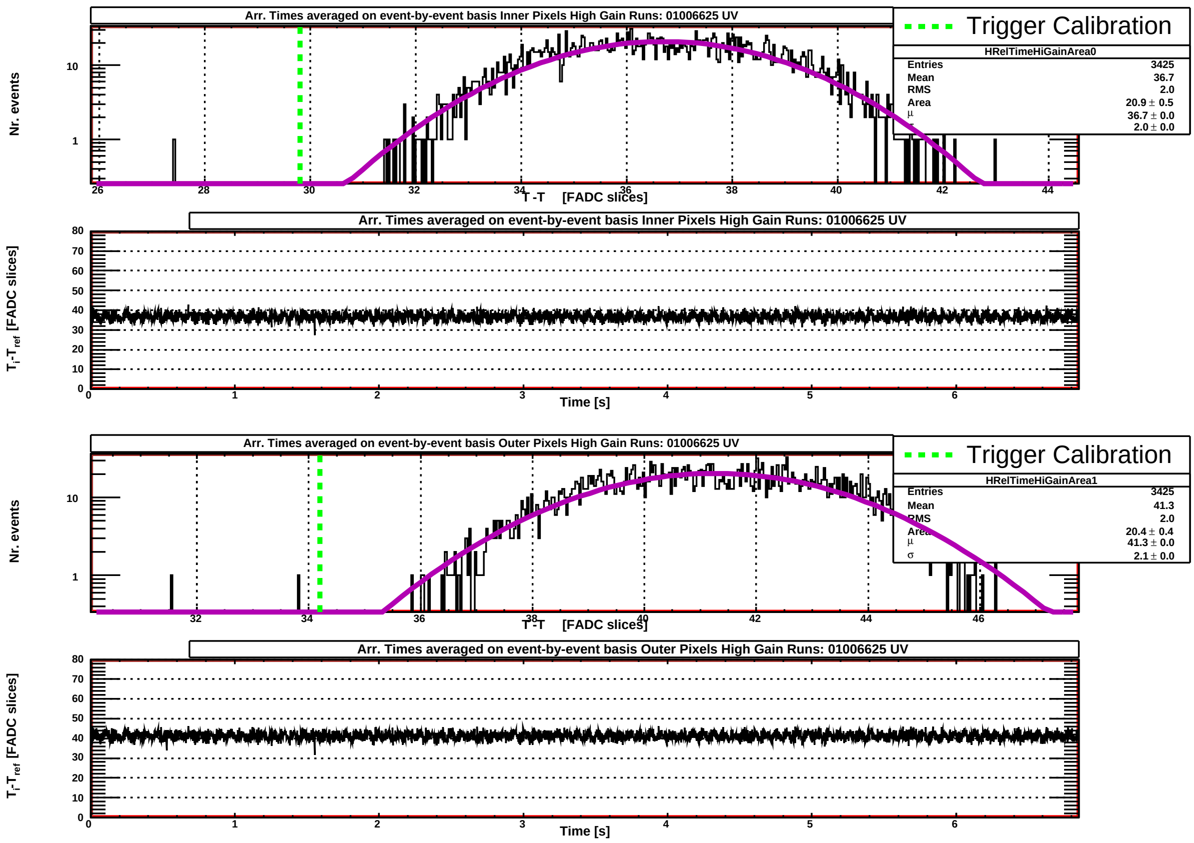

Figure 34: *Mean arrival time (FADC slice). From top to bottom: mean arrival time distribution for inner pixels (first 2 plots) and outer pixels (last 2 plots). The second and fourth plot show this arrival time parameter versus time (sec) during the calibration run, which lasts a few seconds, for both inner and outer pixels.*

Calibration signal charge Figure 35 shows the distribution of the calibration signal mean charge (in FADC counts) and its behaviour versus time (sec) for inner and outer pixels. A reference line with the charge of the corresponding calibration script (values "{Inner/Outer}RefCharge" of the MJCalibration.ReferenceFile) is plotted on it.

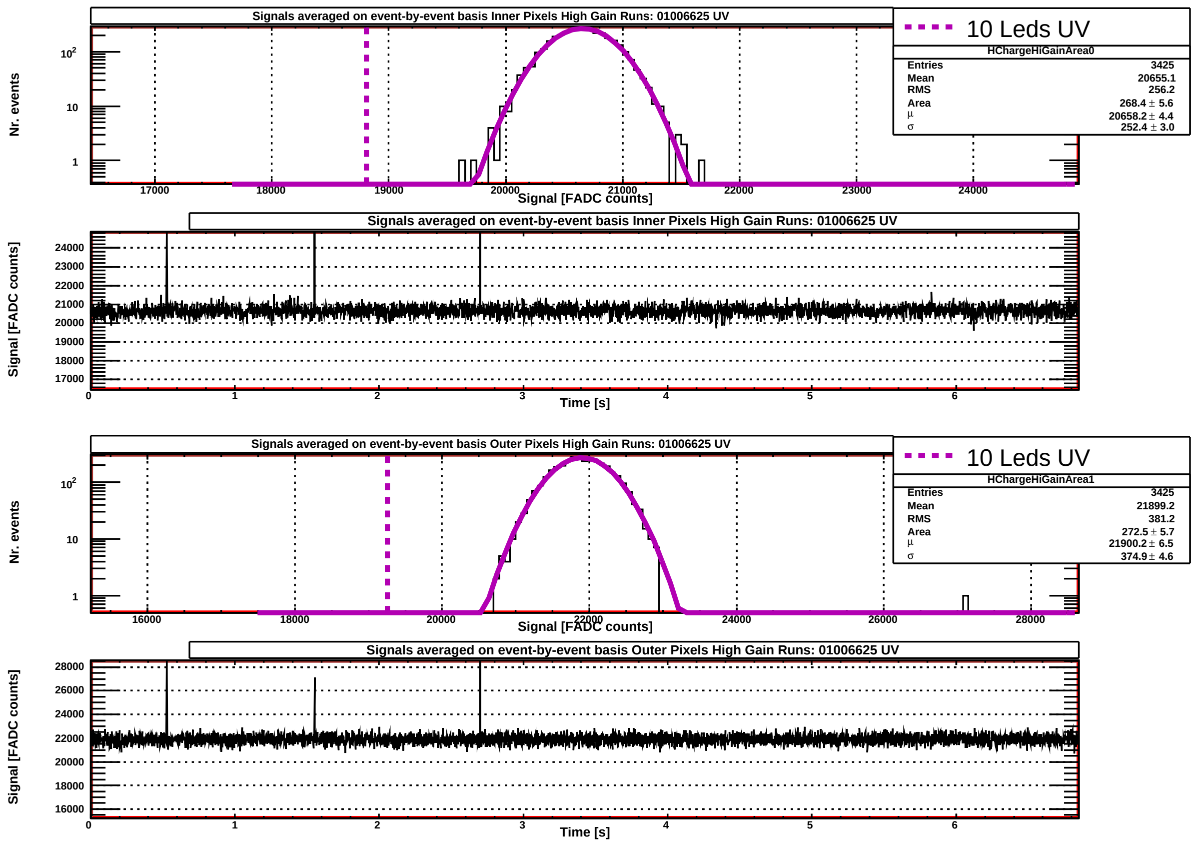

Figure 35: *Calibration signal charge (FADC counts). From top to bottom: mean calibration signal charge (FADC counts) distribution for inner (first 2 plots) and outer pixels (last 2 plots). The second and fourth plot show this mean charge versus time (sec) during the calibration run for both inner and outer pixels. The reference lines correspond to the expected light for the specific calibration script.*

Fitted charge In figure 36 the mean (in FADC counts) and RMS of the fitted signal charge versus camera pixel number is plotted as a profile and as a camera display. It also shows the distribution of the fitted mean charge, quantifying the number outlier pixels (too low or too high charge) and the flat-field precision. Finally, the charge RMS and Npe RMS distributions are shown (for inner and outer pixels) with the number of dead and noisy pixels. The low amplification and high amplification as well as the dead and noisy pixels are the integral of the distributions at $\pm\, 4\sigma$ of the fitted distribution. The flat-field precision is defined as the σ of the gaussian fit of the charge divided by the mean from the same fit, and multiplied by a factor 100. The number of photo-electrons is computed by the F-factor method.

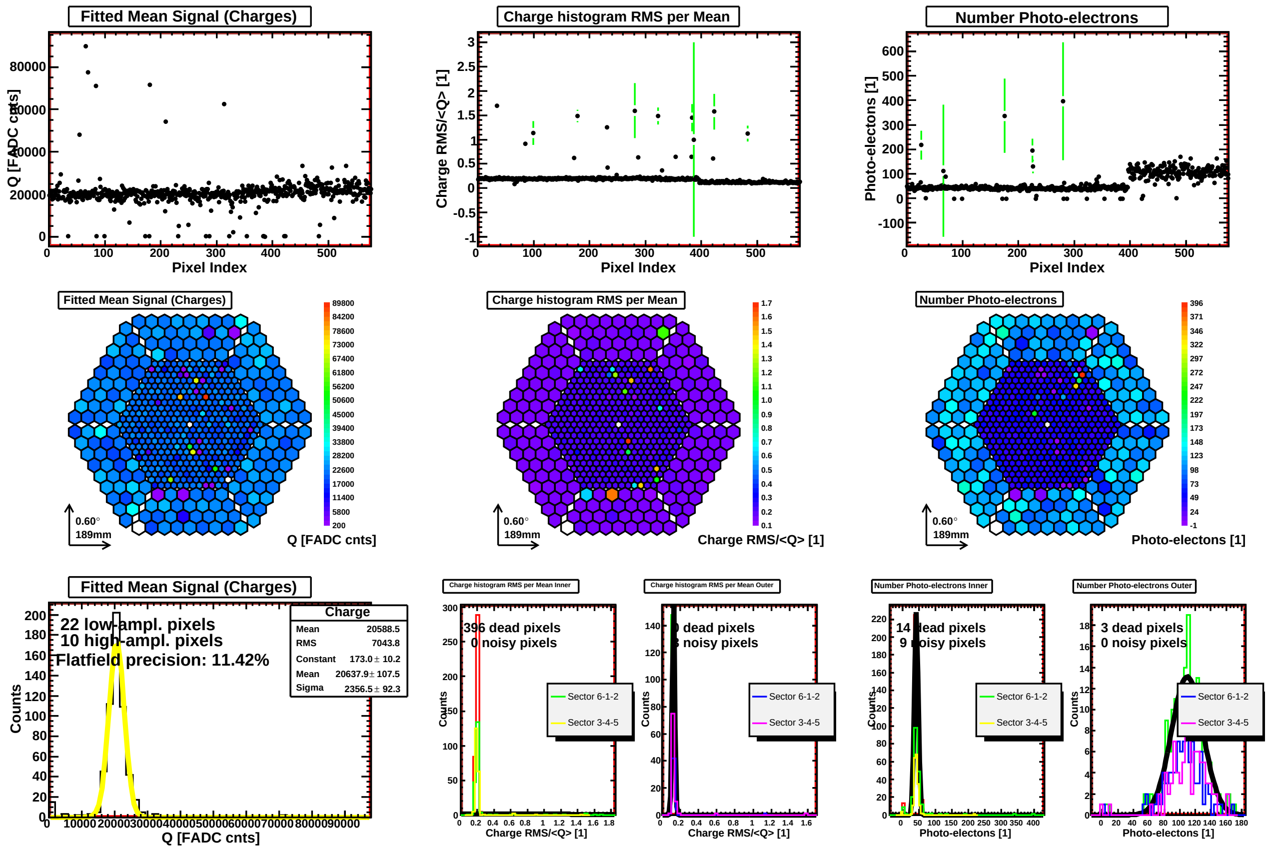

Figure 36: *Fitted charge (FADC counts) and Npe. From top to bottom: the average versus pixel index as profile and camera display, and the distribution for the following variables: fitted mean charge and RMS, and the Npe.*

Conversion factor Figure 37 shows the average value of the conversion factors from charge to equivalent Npe versus pixel number in profile and camera display views, and the distribution (inner and outer pixels) of this calibration constant, obtained using the F-factor method. [14].

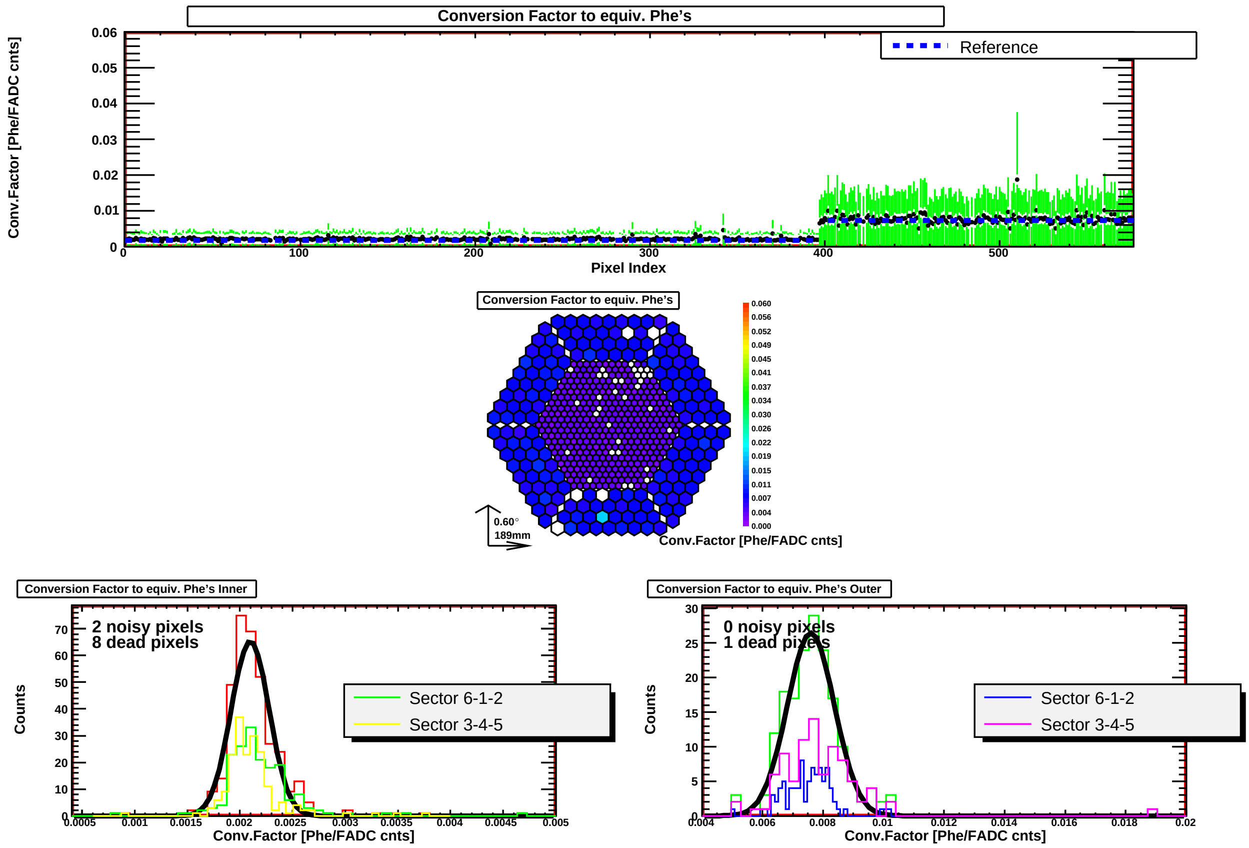

Figure 37: *Conversion factors from FADC counts to Npe. From top to bottom: the average value versus pixel index as profile and as a camera display, and the distribution for the number of the conversion factor.*

The reference lines correspond to the reference default values at callisto.rc in [14] (MJCalibration.ReferenceFile on "callisto.rc").

Absolute times Figure 38 shows the mean and RMS values of the arrival FADC slice of the calibration events versus pixel number in a profile and camera display views. It also displays the distribution of the RMS for inner and outer pixels together with the corresponding number of outliers: "early" and "late" pixels (pixels at $\pm 4\sigma$ of the fitted mean of the mean arrival time per pixel) and "too stable" and "jittering" pixels (at $\pm 4\sigma$ of the average of the mean arrival time rms). For the plots showed here, the pulse peak position has been used to determine the arrival time position.

The reference lines correspond to the reference default values "RefArrivalTime{Inner/Outer}" and "RefArrivalTimeRms{Inner/Outer}" (MJCalibration.ReferenceFile on "callisto.rc").

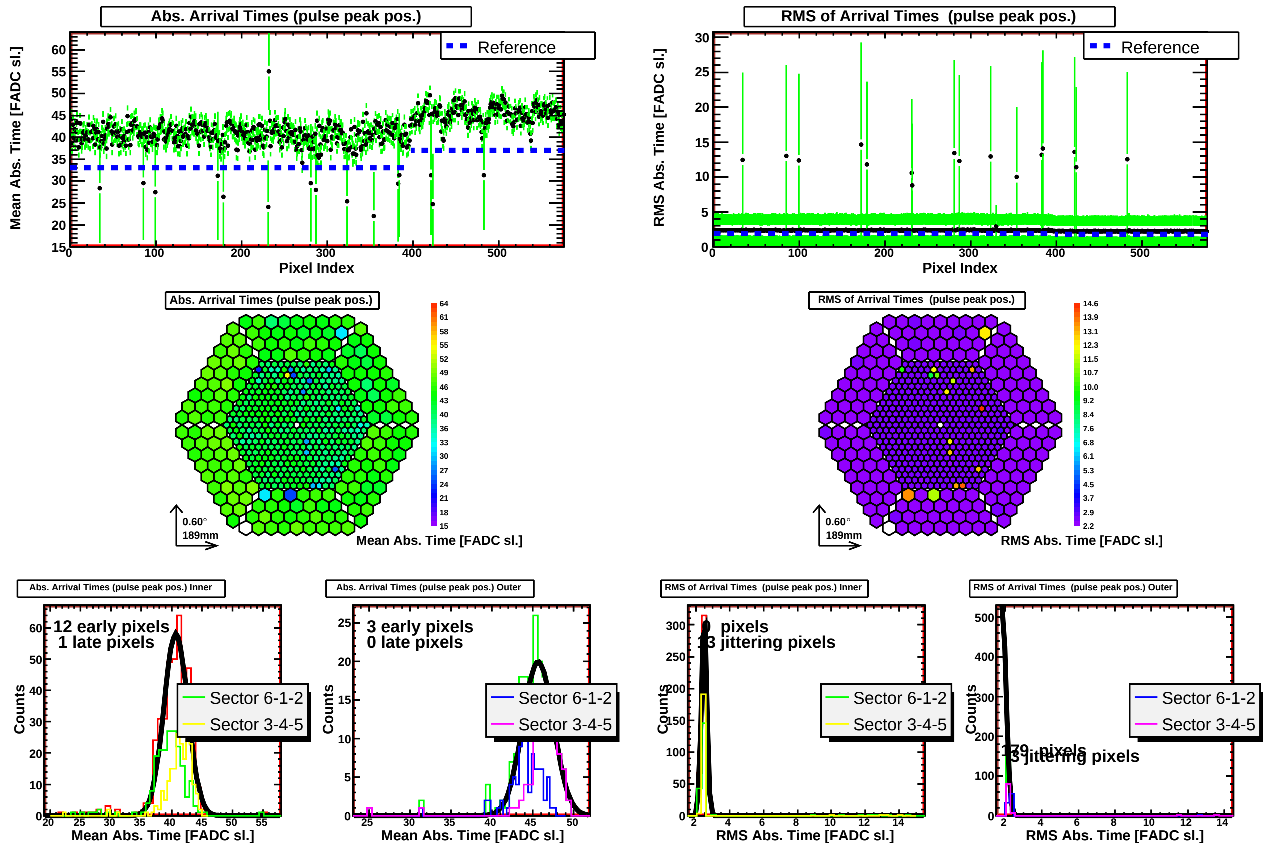

Figure 38: *Arrival times (FADC slice). From top to bottom: Mean and RMS of arrival FADC slice in profile and camera display and their distributions (for inner and outer pixels).*

Defective pixels Figure 39 shows the defective pixels found in the calibration process. A legend is shown with the criteria (in different colors) to classify the pixels into "non suited" and "non reliable" pixels [9]. They are shown with the same color criteria in a camera display.

The pixels marked as "non suited" are not used in the further analysis to build the images, while the "non reliable" pixels will be replaced in the image cleaning analysis process by the mean signal of their surrounding neighbors.

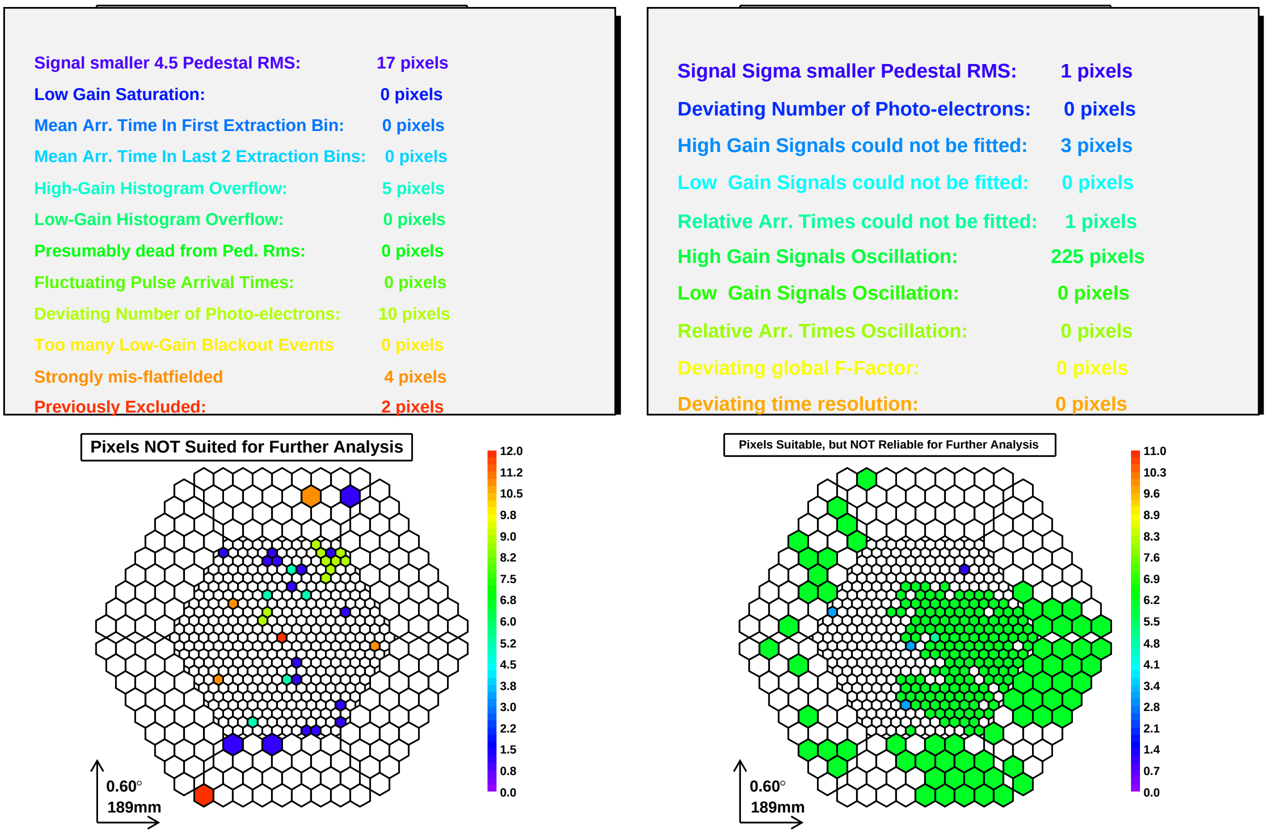

Figure 39: *Defective pixels. Legend with information about the calibrated defective pixels and a camera display showing the corresponding pixels, with colors indicating the kind of defect. On the left the "non suited pixels" and on the right the "non reliable" pixels.*

Relative times Figure 40 displays the mean time delay (FADC slice) and its RMS per pixel in a profile and camera display. The relative arrival times are calculated with regard to pixel number 1 (hardware number = 2). The distribution of the camera mean and RMS for inner and outer pixels is also shown with the number of early and late pixels, and the "too stable" and "jittering" pixels. .

The reference lines correspond to the reference default values "RefTimeOffset{Inner/Outer}" and "RefTimeResolution{Inner/Outer}" (MJCalibration.ReferenceFile on "callisto.rc").

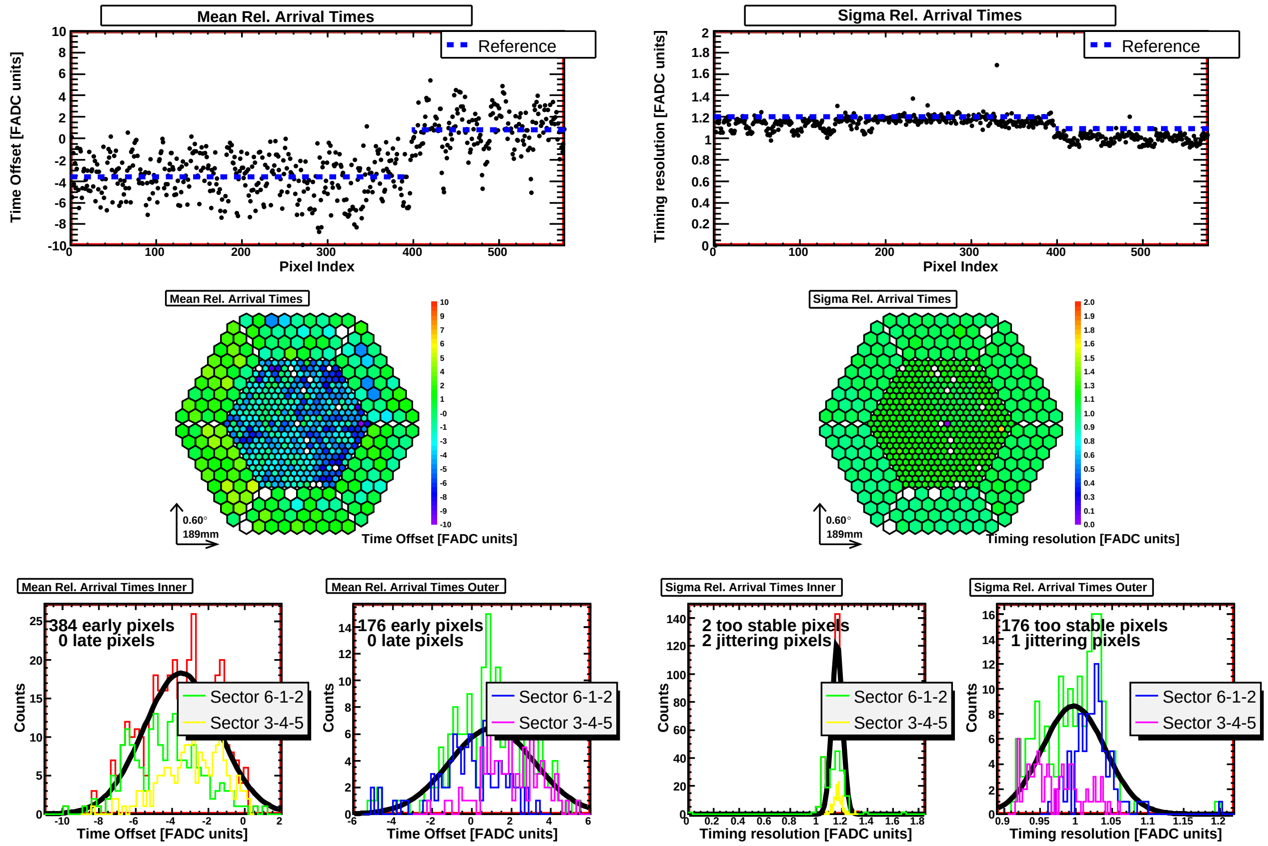

Figure 40: *Relative arrival time (FADC slice). From top to bottom: mean and RMS of relative arrival FADC slice in profile and camera display and their distributions (for inner and outer pixels).*

2.4.4 PC-Rubidium clock time plots

The synchronization between GPS and Rubidium clock is only performed for under-second time scales. It may be that there is a mismatch of exactly 1s multiples between them. In order to detect super-second mismatches, figure 41 displays the distribution of time differences between PC and the rubidium clock, with one entry per run. It is obtained comparing the run start time (from the PC, synchronized over Internet) with the time of the first event (time from the rubidium clock). A difference of less that 1 second means that the system is synchronized. Figure 42 displays the evolution along the night, in terms of the run number of this time difference.

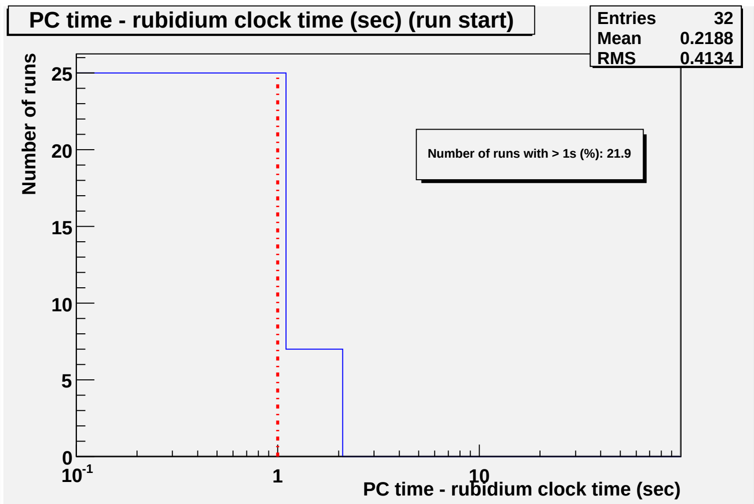

Figure 41: *Distribution of the time difference between the PC and the rubidium clock. The red dashed reference line is 1 second of time difference*

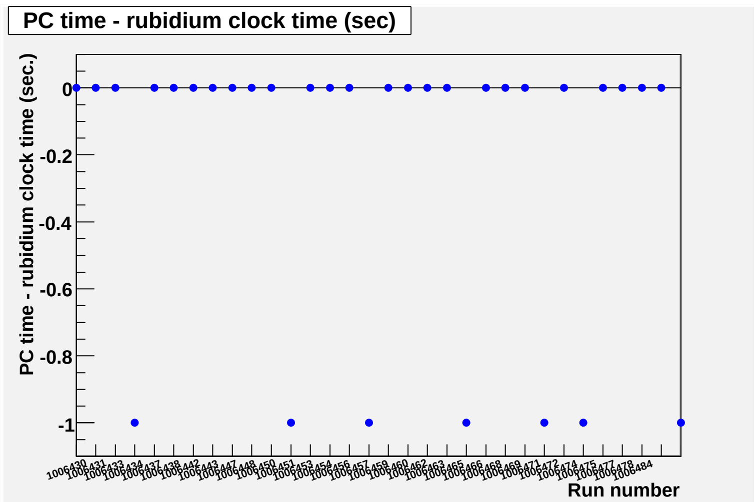

Figure 42: *Evolution plot of the time difference between the PC and the rubidium clock. One value of the time difference is obtained per each data run*

2.4.5 Arrival time distributions for all events

The following distributions are obtained using the arrival times obtained directly from the pixels of individual events. In order to speed up the process but to have a significant sample of data, 10% of all the events of the data taking night are used, selected randomly and according to the type of event. Figure 43 shows the arrival times obtained from calibration pulses of calibration runs, whereas figure 44 shows the arrival times from calibration interleaved events. The calibration pulses are not yet calibrated: This means that the arrival times are pure arrival times without correction for the differences in cable lengths and PMT transit times. The calibration of the arrival times is performed later, during the calibration, using as reference the arrival time of the pixel hardware number 2 (the effect of the arrival time calibration can be seen at figure 40). The number of photo-electrons are estimated as signal charge, multiplied with a global estimation of the conversion factor.

The remaining arrival times are already calibrated as explained above. Figures 45 and 46 show the arrival time distributions for trigger level 1 events and sum trigger events respectively. Finally, Figure 47 displays the arrival time for all events those of calibration runs.

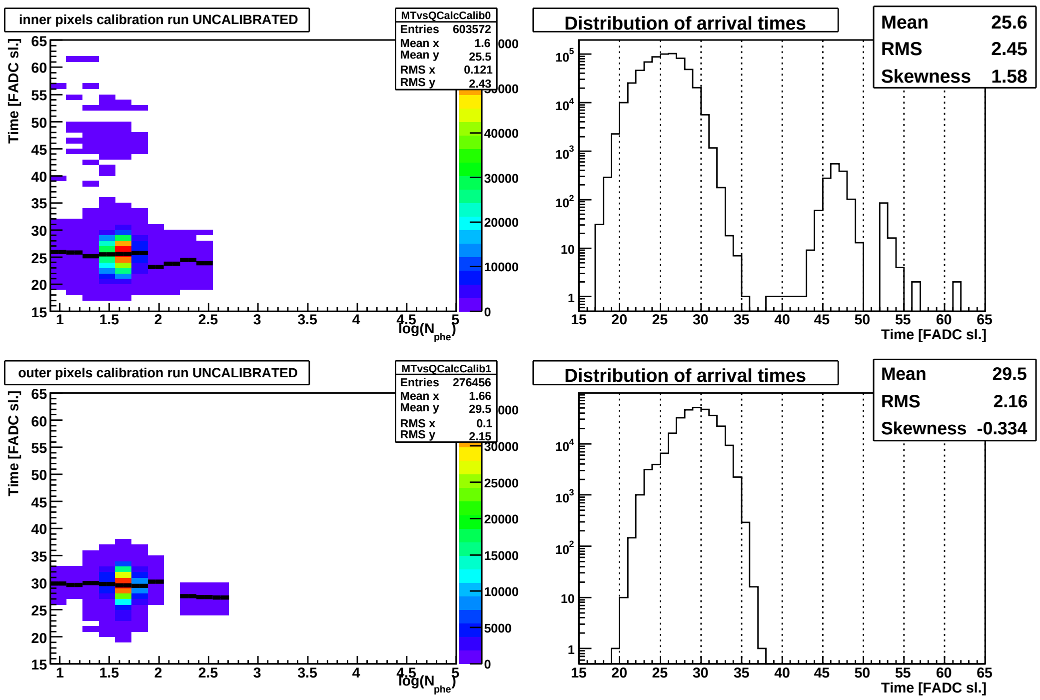

Figure 43: *Size dependant and overall distributions of calibration pulses, for calibration runs, from both inner and outer pixels.*

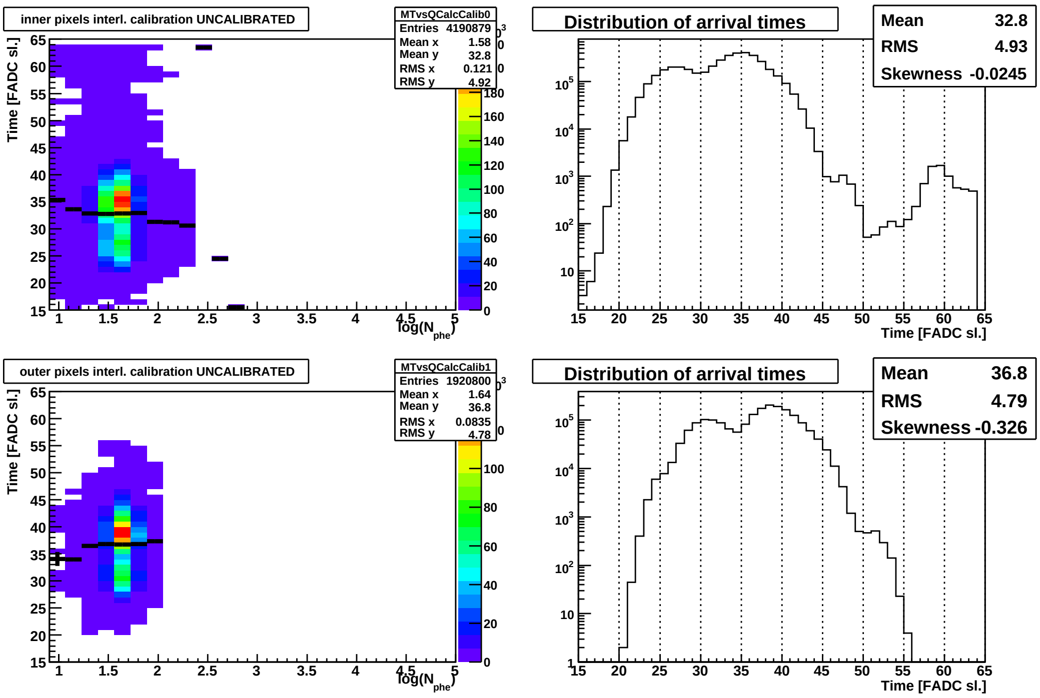

Figure 44: *Size dependant and overall distributions of interleaved calibration pulses, from data runs, for both inner and outer pixels.*

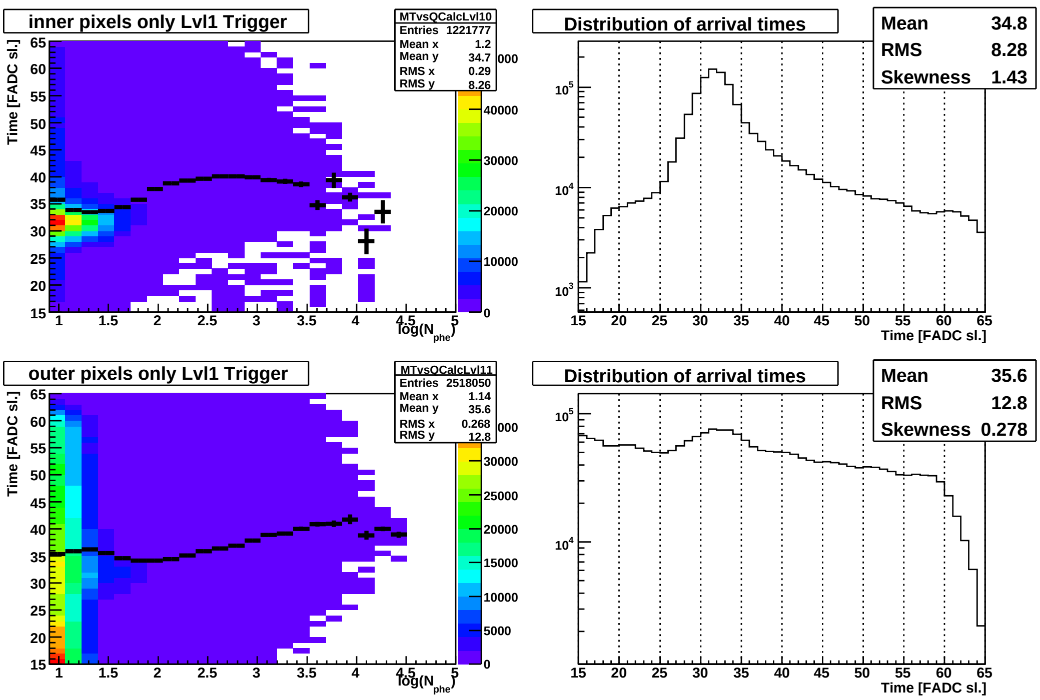

Figure 45: *Size dependant and overall distributions of level 1 trigger events for both inner and outer pixels.*

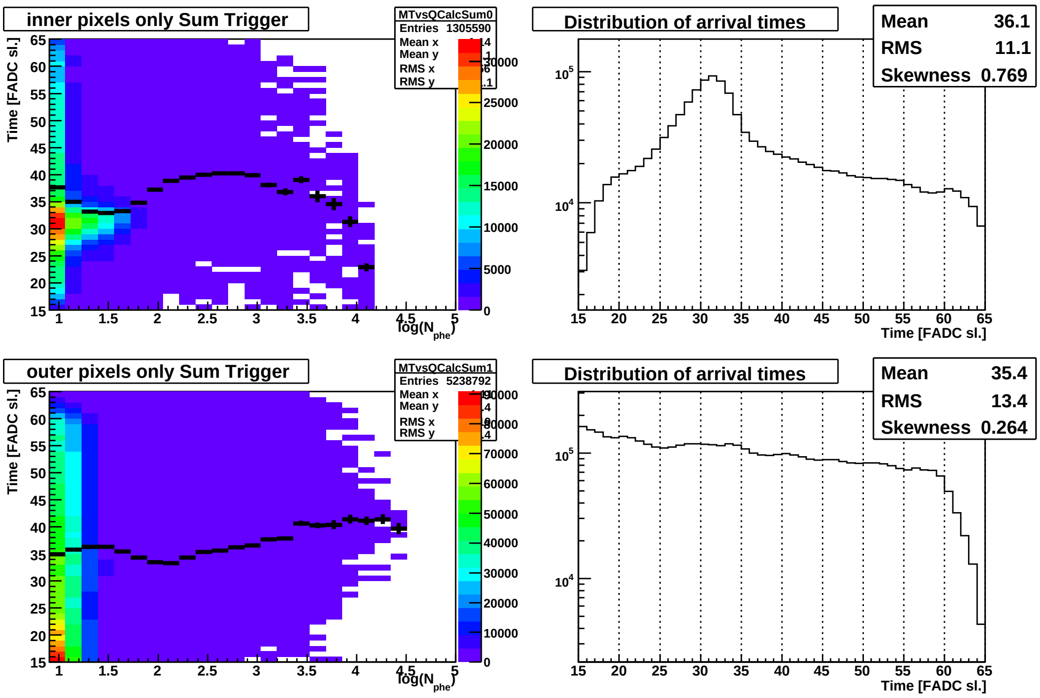

Figure 46: *Size dependant and overall distributions of sum trigger events for both inner and outer pixels.*

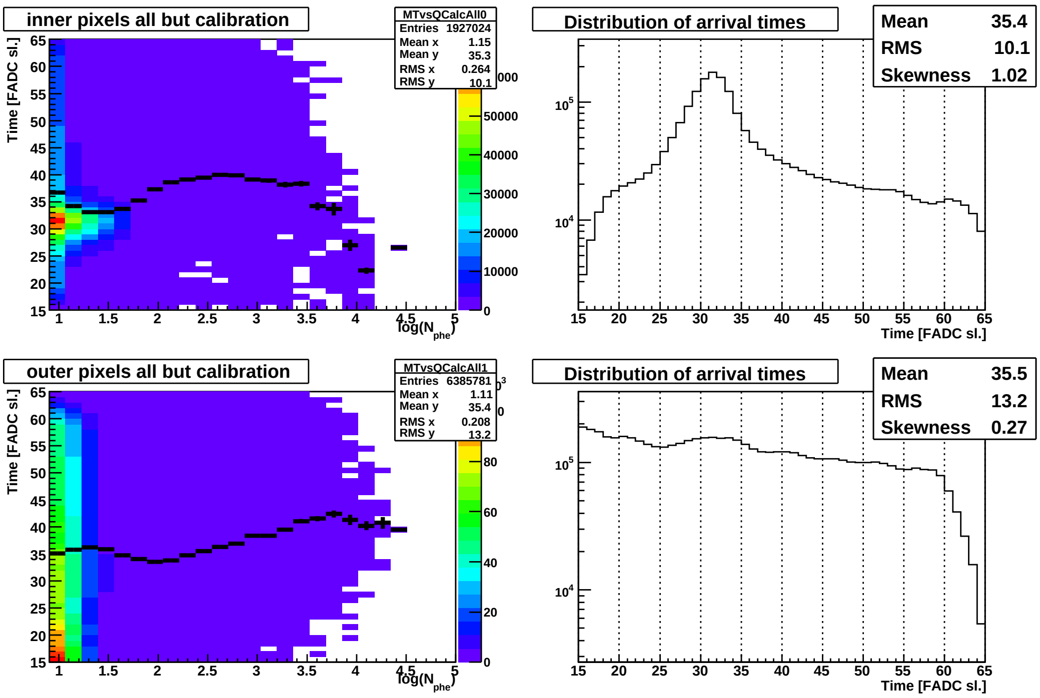

Figure 47: *Size dependant and overall distributions of all events except calibration ones, for both inner and outer pixels.*

2.5 Analysis data check

The image parameters of the Cerenkov showers can be used to give an additional estimation of the night data quality. Profiting from having available the on-site analysis products in the same computing cluster, we can evaluate the image parameters for all the data taken during the night.

2.5.1 Program

The input files for this job are the Hillas [11] and others image parameters obtained in the regular star processes from the on-site analysis. As described at reference [15], the on-site analysis runs the *star* MARS executable over all data runs of the data taking night. Each time *star* is run, an output *star.root* file is generated. This output file contains all relevant parameters obtained from the images of the showers. The on-site analysis script *littlesequence.csh*, that takes care of processing each sequence, also launches the *GetHillas.C* root macro. This root macro gets the image parameters from the *star.root* files. The input and output files are copied at the directory
/mnt/raid2/analysis/DataCheck/Data/hillas/<year>_<month>/<year>_<month>_<day>/.
Finally, *littlesequence.csh* also copies of the output .pdf files to the webpage at La Palma.

2.5.2 Plots

The following plots show the image parameters after the image cleaning performed with the so-called *absolute time image cleaning*. The configuration is the MARS default one: absolute 6/3 photo-electrons for core/boundary pixels, 4.5 ns maximum time difference between mean core pixels arrival times and single core pixels arrival times, and 1.5 ns maximum time difference between a boundary pixel arrival time and its core pixel neighbor arrival time. More details on the used image cleaning can be found in reference [1]. An independent set of plots is created from each different source, two plots per source if the observation has been carried out in wobble mode.

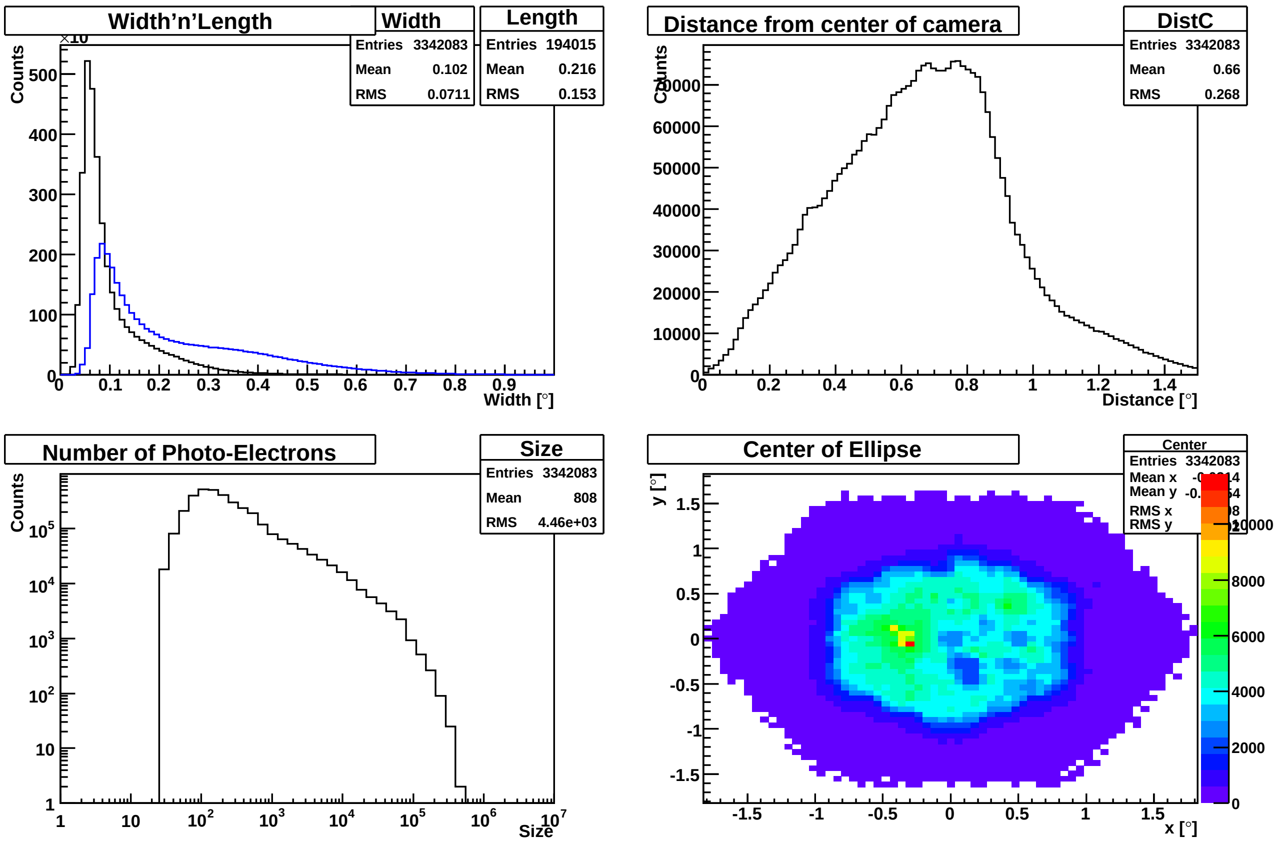

Figure 48: *Hillas parameters. Top left: length and width (deg), defined as the second moments of the image. Top right: distance from the center of the ellipse to camera center (deg). Bottom left: Size, defined as total number of photo-electrons after the image cleaning. Bottom right: CoG of the center of the ellipse (deg).*

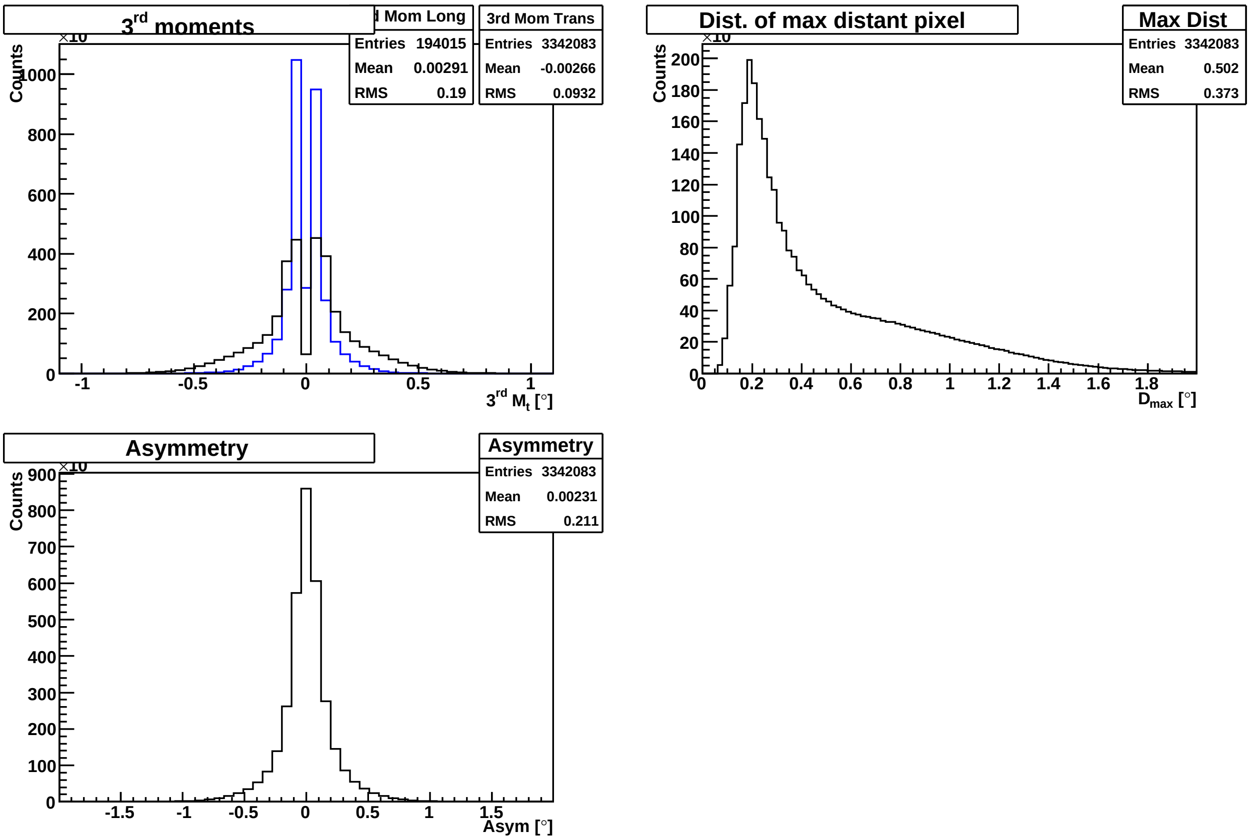

Figure 49: *Extended image parameters. Top left: Longitudinal and transverse third moments of the image (deg). Top right: distance from most distant used pixel to camera center (deg). Bottom left: Distance from the pixel with more number of photo-electrons to center, projected onto major axis, (deg).*

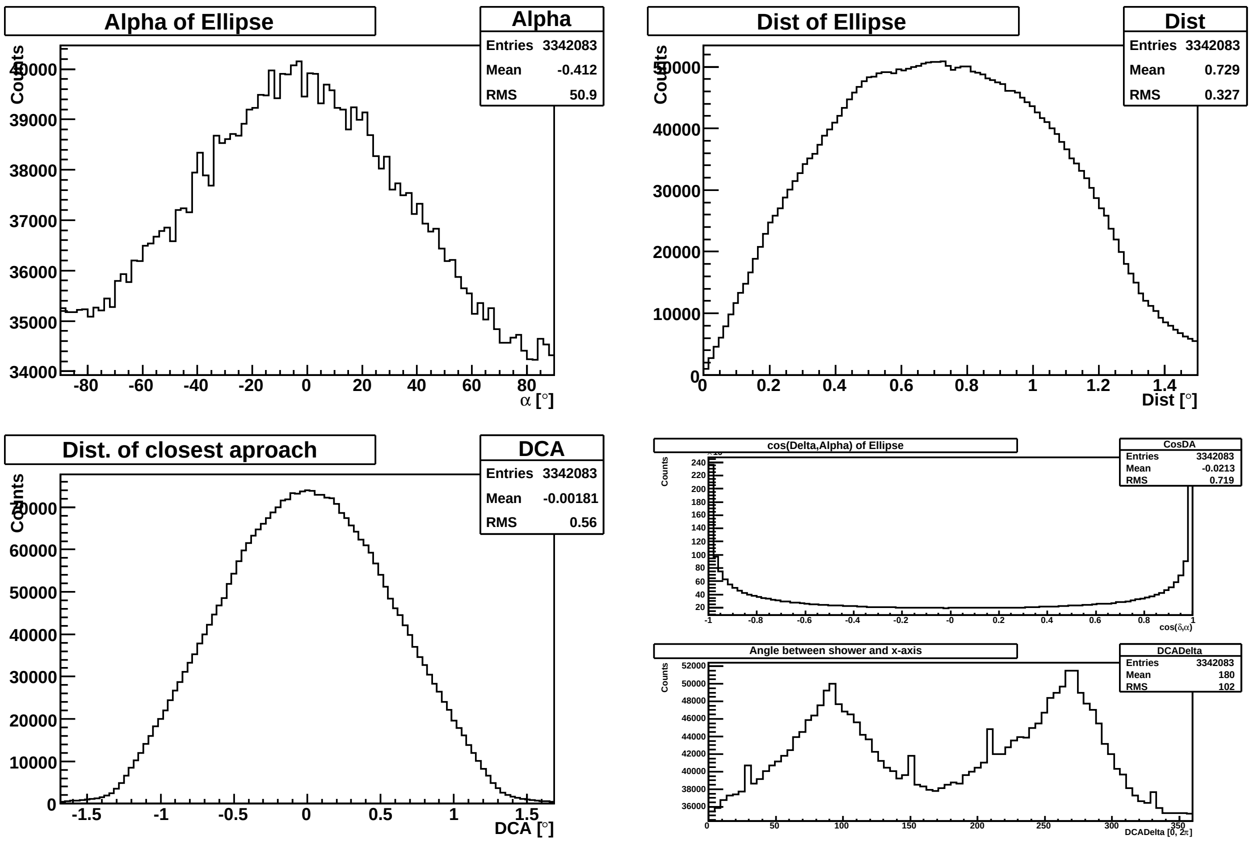

Figure 50: *Source-dependent image parameters. Top left: angle between major axis and the line source-to-center. Top right: distance from the source position in the camera to the center of Hillas ellipse. Bottom left: Distance to closest approach. Bottom right: cosine of angle between d and a, where d is the vector from the source position to the center of the ellipse a is a vector along the main axis of the ellipse, defined with positive x-component and angle of the shower axis with respect to the x-axis.*

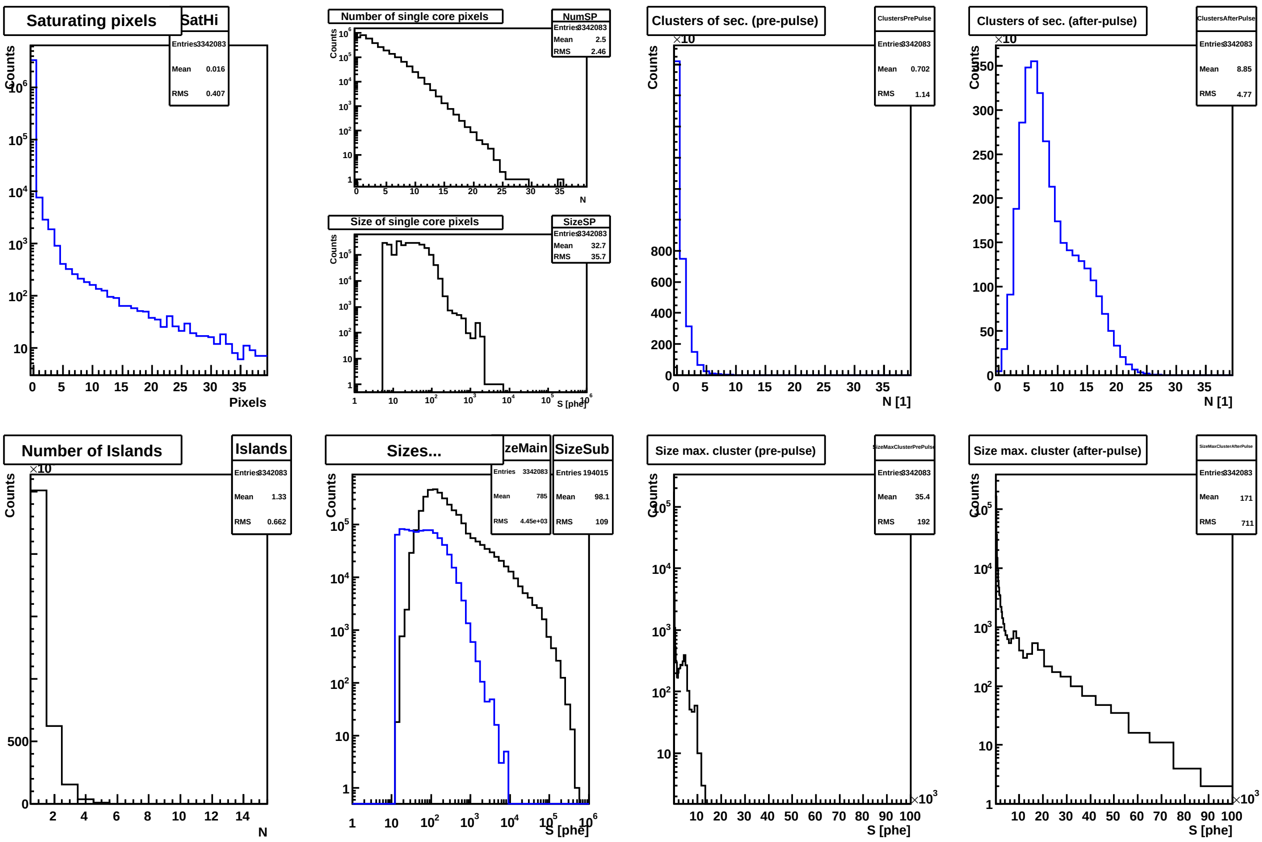

Figure 51: *Image parameters. Top, from left to right: number of pixels with saturating gains, number of single core pixels and their size, number of clusters from secondaries pre-pulse, number of clusters from secondaries after-pulse. Bottom, from left to right: number of islands found, sizes of primary and secondary islands in photo-electrons, size of maximum cluster from secondaries pre-pulse in photo-electrons and size of maximum cluster from secondaries after-pulse in photo-electrons.*

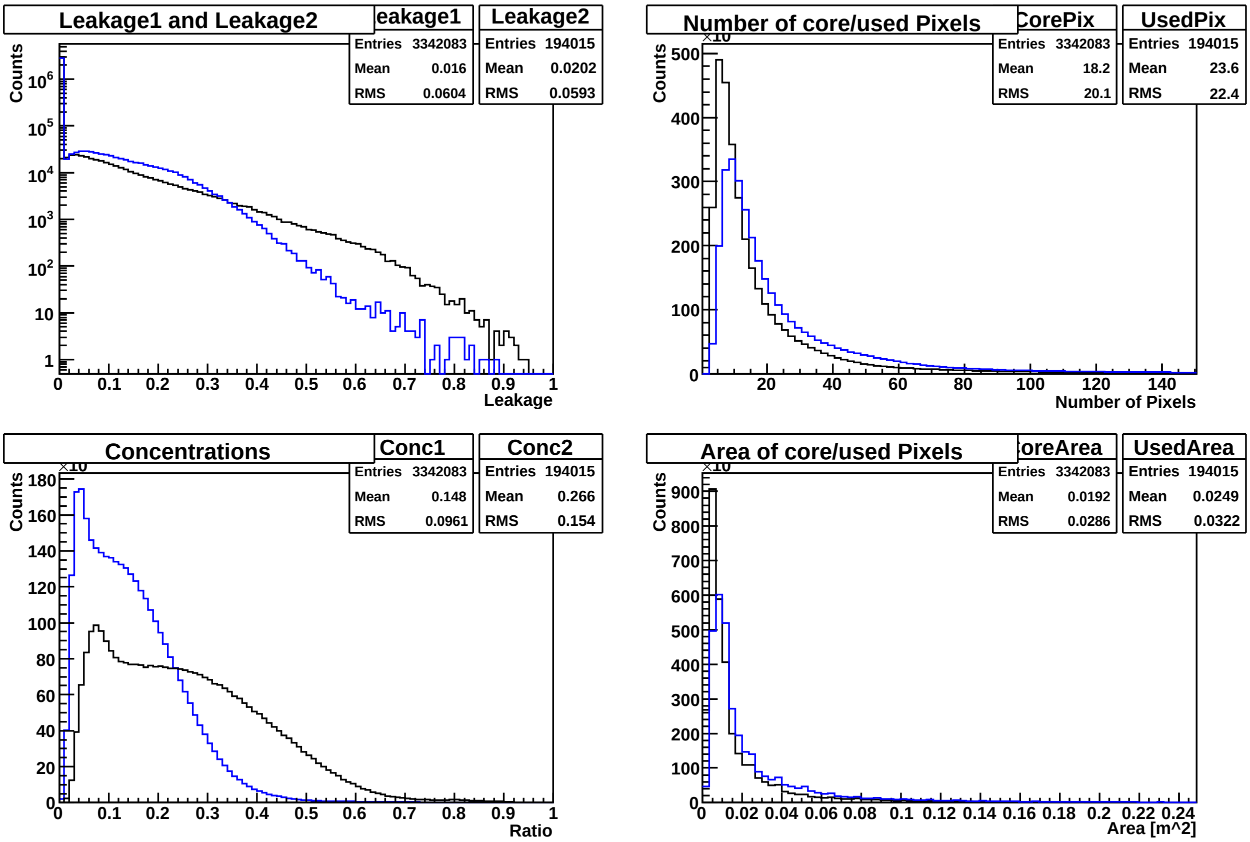

Figure 52: *More image parameters. Top left: Leakage1, defined as measured number of photo-electrons in outermost ring of pixels over total size of the image, and leakage2, identically defined but for the 2 outer rings. Top right: Number of pixels which survived the image cleaning and number of core pixels. Bottom left: Concentration ratio 1, defined as the number of photo-electrons of the highest pixel over the size of the image, and Concentration ratio 2, defined identically but for the two highest pixels. Bottom right: Area of pixels which survived the image cleaning and area of core pixels, both in* m^2.

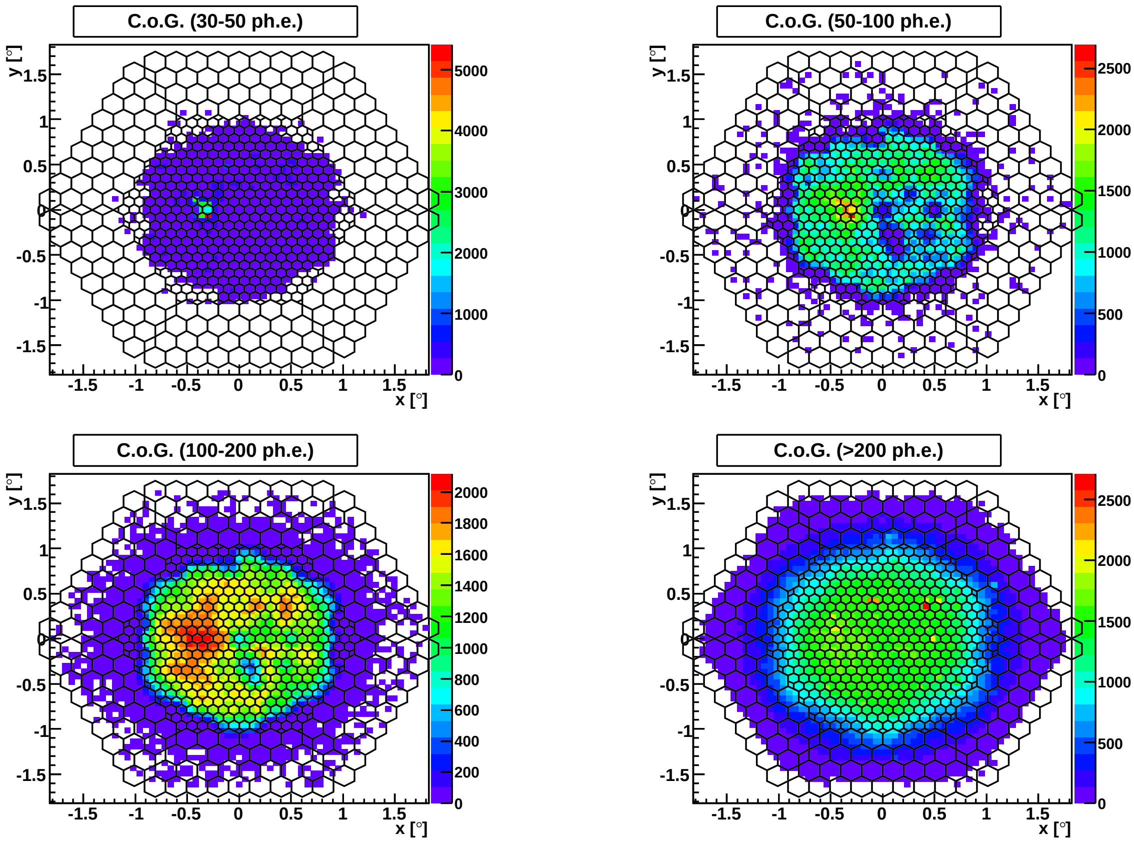

Figure 53: *Inhomogeneity. Center of gravity of the cleaned image (deg) for different size bins.*

2.6 Automatic data check

The automatic data check program evaluates a set of the most important plots in order to detect any possible defective working subsystem. It fills a form later on completed by human supervision checking only two plots with suspected problems.

After the human supervision a mail report is sent to the whole MAGIC collaboration while, if any important problem is spotted, experts are contacted by the person in charge of the daily check. A detailed explanation of the daily-checker duties can be obtained at [6]

2.6.1 Program

The part of the MAGICDC program which evaluates the previously obtained results is called by the script *AUTODATAChecking*. This script calls a root-macro, *daily.C*, to read the previously created .root files at cc, daq and calibration jobs. The macro will evaluate the different parameters in the previously described plots and generate an ASCII file with the results of the evaluation: <year>_<month>_<day>autocheckv2.txt.

The log file of *AUTODATAChecking* job, named AUTODataChecking_<year>_<month>_<day>.out, is copied, together with the program results, into the directory /remote/raid2/analysis/DataCheck/Data/auto/<year>_<month>/<year>_<month>_<day>/.

The daily check form is filled at PIC www.magic.pic.es/priv/dailycheck/. A copy of the questions are stored at the data check webpage at La Palma http://www.magic.iac.es/operations/datacheck/WWW/dailycheck.txt.

3 Program report and outlook

Since its installation on January 2004, the data check program has been improved and the number of subsystems to check has increased and therefore the number of plots. The increase has been due to the addition of new reports to the central control, improvements in the software and, most of all, the feedback from users and system responsibles about known/unknown new subsystem features.

The union of this program, together with the ON-SITE ANALYSIS, allows us to know any system failure before 11:00 UTC and, whether everything has gone right, to have a first standard analysis of night data before 12:00 UTC.

In the coming future there are plans to perform more improvements for the optimization of the program itself:

- Keep going on with the software update for MAGIC-II and the system of the two telescopes.
- Make a long term study of the telescope parameters.

Finally we would like to thanks all of you for your comments and suggestions that have helped to the program improvement and very specially to those involved more directly in any part of the program development: J.A. Barrio, J.A. Coarasa, J. Cortina, R. Firpo, M. Gaug, F. Goebel, P. Majumdar, A. Moralejo, D. Mazin and T. Schweizer.

List of Figures

References

[1] E. Aliu et al., *Improving the performance of the single-dish Cherenkov telescope MAGIC through the use of signal timing* , Astropart. Phys. 30 (2009) 293

[2] J. Albert et al., *FADC Signal reconstruction for the MAGIC telescope* J. Albert et al., Nucl. Instr. Meth. A 594 (2008) 407.

[3] Bartko H. et al, 2005, *Comparison of Signal Reconstruction Algorithms for the MAGIC Telescope*, MAGIC internal documentation, TDAS 05-03.

[4] Carmona E. et al., 2009, *A Flexible High Demand Storage System for MAGIC-I and MAGIC-II using GFS*, 31st ICRC, Lódź, Poland.

[5] Coarasa J.A., 2005, *Online PC Farms for MAGIC-II and Data Transfer*, MAGIC Collaboration Meeting, Tenerife.

[6] Cortina, J., Oya, I. 2006, *DailyCheck Manual* , MAGIC internal documentation, TDAS 06-02.

[7] De los Reyes, R. , PhD Thesis, Universidad Complutense de Madrid, July 2008. http://magic.mppmu.mpg.de/publications/theses/index.html

[8] Flix Molina J., PhD Thesis, Universitat Autonoma de Barcelona, April 2006. http://magic.mppmu.mpg.de/publications/theses/index.html

[9] Gaug M. , PhD Thesis, Universitat Autonoma de Barcelona, March 2006. http://magic.mppmu.mpg.de/publications/theses/index.html

[10] Goebel F., 2005, *Users guide and reference manual for the Data Acquisition and the FADC system of the MAGIC telescope*, MAGIC internal documentation, TDAS 04-01.

[11] Hillas A.M., 1985, *Cherenkov Images of EAS produced by primary gamma rays and by nuclei*, Proc. 19th ICRC (La Jolla), 3, 445.

[12] http://cvs.ifae.es/cgi-bin/viewcvs.cgi/MagicSoft/MAGICDC/

[13] http://www.magic.iac.es/operations/datacheck/

[14] http://magic.pic.es/priv/cvs/ (MAGIC private URL)

[15] Nieto D., et al, 2009, *On-site analysis of the MAGIC telescope*, MAGIC internal documentation, TDAS 09-06-2.

[16] http://magic.pic.es/ (MAGIC private URL)

[17] http://www.magic.iac.es/operations/datacheck/docu_dcheck.pdf (MAGIC private URL)

[18] http://www.magic.iac.es/site/weather/

[19] Meyer M., 2005, *Calibration of the MAGIC telescope using muon rings*, MAGIC internal documentation, TDAS 05-10.

[20] Oya, I., Diploma thesis, UCM, September 2006.

[21] Reichardt et al., 2009, *The MAGIC data center*, 31st ICRC, Lódź, Poland.